



Systematic development of a high dosage formulation to enable direct compression of a poorly flowing API: a case study

Barbara E. Schaller, Kevin M. Moroney, Bernardo Castro-Dominguez, Patrick Cronin, Jorge Belen-Girona, Patrick Ruane, Denise M. Croker, Gavin M. Walker

Publication date

01-01-2019

Published in

International Journal of Pharmaceutics;566, pp. 615-630

Licence

This work is made available under the [CC BY-NC-SA 1.0](#) licence and should only be used in accordance with that licence. For more information on the specific terms, consult the repository record for this item.

Document Version

2

Citation for this work (HarvardUL)

Schaller, B.E., Moroney, K.M., Castro-Dominguez, B., Cronin, P., Belen-Girona, J., Ruane, P., Croker, D.M. and Walker, G.M. (2019) 'Systematic development of a high dosage formulation to enable direct compression of a poorly flowing API: a case study', available: <https://hdl.handle.net/10344/8323> [accessed 24 Jul 2022].

This work was downloaded from the University of Limerick research repository.

For more information on this work, the University of Limerick research repository or to report an issue, you can contact the repository administrators at ir@ul.ie. If you feel that this work breaches copyright, please provide details and we will remove access to the work immediately while we investigate your claim.

Systematic development of a high dosage formulation to enable direct compression of a poorly flowing API: A case study

Barbara E. Schaller¹, Kevin M. Moroney^{1,2}, Bernardo Castro-Dominguez³, Patrick Cronin¹,
5 Jorge Belen-Girona⁴, Patrick Ruane⁴, Denise M. Croker¹, Gavin M. Walker¹

¹*Synthesis and Solid State Pharmaceutical Centre (SSPC), Bernal Institute, University of Limerick, Limerick, Ireland.*

²*MACSI, Department of Mathematics and Statistics, University of Limerick, Limerick, Ireland.*

10 ³*Chemical Engineering Department, University of Bath, Claverton Down, BA2 7AY Bath, United Kingdom.*

⁴*Johnson & Johnson Supply Chain, Product Supply – Manufacturing Engineering and Technology.*

Abstract

15 In this work, the transfer of oral solid dosage forms, currently manufactured via wet granulation, to a continuous direct compression process was considered. Two main challenges were addressed: (1) a poorly flowing API (Canagliflozin) and (2) high drug loading (51 wt%). A scientific approach was utilised for formulation development, targeting flow and compaction behaviour suitable for manufacturing scale. This was achieved through systematic screening of excipients to identify
20 feasible formulations. Targeted design of experiments based on factors such as formulation mixture and processing parameters were utilised to investigate key responses for tablet properties, flow and compaction behaviour. Flow behaviour was primarily evaluated from percentage compressibility and shear cell testing on a powder flow rheometer (FT4). The compaction behaviour was studied using a compaction simulator (Gamlen). The relationships between tablet porosity, tensile strength and
25 compaction pressure were used to evaluate tableability, compactibility and compressibility to assess scale-up. The success of this design procedure is illustrated by scaling up from the compaction simulator to a Riva Piccola rotary tablet press, while maintaining critical quality attributes (CQAs). Compactibility was identified as a suitable scale-up relationship. The developed procedure should allow accelerated development of formulations for continuous direct compression.

Abbreviations: Run # = run number of DoE; FF = flow function; CP% = compressibility percentage; CBD = conditioned bulk density; σ_t = tablet tensile strength; D_t = disintegration time; ε = porosity; P_y = mean yield pressure; ER_0 = immediate elastic recovery; ER_{48} = elastic recovery after 48 hours; $d_{10}/d_{50}/d_{90}$ = Particle size distribution

30 **Keywords:** Continuous direct compression, raw material characterization, systematic formulation development, high dosage formulation, compactibility, flow and compaction behaviour.

1 Introduction

The manufacture of oral solid dosage forms (OSD) can be achieved using a number of processing pathways of differing cost and complexity. The simplest and most cost-effective route is the direct
35 compression process (DC). In comparison to more complicated processes, such as dry granulation (DG) and wet granulation (WG), DC offers reduced cost of equipment, faster processing and a simple and efficient process path [1]. Unfortunately, many products, particularly those with a high loading of active pharmaceutical ingredient (API), are very difficult to process into tablets by direct compression. The main reasons for this are poor flow or compression properties of the API and/or
40 excipient mixture [2, 3]. Many of these products are manufactured using a WG process. Thus, there is significant benefit in the transition of a drug product from a WG process to a DC process.

Implementing a continuous direct compression process has further advantages over traditional batch processes, including scale-up benefits, reduced batch-to-batch variability, reduced production costs, reduced footprint for the manufacturing facility and faster product release [1, 4]. While direct
45 compression is an inherently continuous processing technique, many of its unit operations including weighing and blending are still performed in batches [5].

Designing a robust DC formulation for an API with poor flow and compaction properties at a high API load is challenging. Physical models relating key flow and compaction responses and product critical quality attributes (CQAs) to fundamental material attributes and process parameters would allow
50 feasibility assessment and optimisation of the process within the design space. However, despite significant research, such quantitative models relating bulk powder performance to particle level properties and process parameters remain elusive. Significant challenges exist in relating behaviour to either (i) the composition of the powder based on the mass percentage of its constituent materials [6] or (ii) some fundamental properties of the powder formulation (particle size
55 distribution and shape, particle roughness, moisture content etc.) [7]. The multivariate nature of the measurement of raw material properties means it is not straightforward to determine which properties influence performance most significantly [7]. Furthermore, flow and compaction properties arise due to a combined effect of material attributes and processing parameters. Thus, commonly used tests for both flow and compaction performance may give different material
60 rankings. Flow behaviour depends on the initial stress state of the powder and equipment interaction [8, 9]. Similarly, compaction responses, such as elastic recovery following tableting, will depend on compaction speed for viscoelastic materials, but not for others [10].

Although there is a large body of research studying specific aspects of powder flow [11 - 17] and compaction [6, 18 - 25] behaviour, comprehensive approaches to formulation design for direct compression remain limited. Several studies consider the implementation of a continuous DC process from a given formulation to the final tablet [4, 5, 26 - 30]. Studies include extended release [5, 27, 28], low dose [30] and immediate release tablets [4, 26]. The most common APIs for these studies were ibuprofen, acetaminophen and naproxen sodium. The studies investigate various aspects of the continuous DC process including variation in blend composition, continuous powder feeding, powder blending and tablet press operation and how these influence product quality. Other studies have focused on specific aspects of the DC process such as resolving poor flow issues in loss-in-weight feeding [30, 31]. While some of these reports consider material properties via multivariate data analysis techniques, such as principle component analysis (PCA) and partial least squares (PLS), the broader issue of formulation design and excipient choice is not considered in detail. Running such tests on a full production line for a variety of excipient choices would be time intensive and consume a significant amount of material, increasing the product development costs. Thus many formulations are still chosen based on the personal experience of formulators and by a trial and error approach [32]. There is a need for a structured scientific approach to formulation design for DC, based on a defined set of material sparing tests, in order to select optimal formulations for scale-up and process optimisation.

A number of lab-scale studies have been performed to evaluate flow and compaction behaviour of direct compression formulations. Tye et al. [33] studied four direct compression formulations and a placebo formulation. They introduced the compaction triangle to study the relationships between compaction pressure, tablet tensile strength and tablet solid fraction in order to evaluate the effects of tableting speed on the produced tablets (USP <1062>)[34]. The relationships between these variables are called tableability, compactibility and compressibility. Assessment of these relationships should allow the determination of whether tablets with an adequate tensile strength at a reasonable porosity can be realised, using an acceptable compaction pressure [33, 43].

Compactibility, the ability of a powder to be transformed into tablets with resulting strength at a given porosity, was proposed as a scale independent relationship, which can be used to predict tensile strength for scale-up. The Ryshkewitch-Duckworth equation [44, 45] has been successfully applied to describe the compactibility behaviour of single powders and also multi-component mixtures using a variety of mixture rules [6, 18, 19]. Tableability defines the capacity of a powder to be transformed into a tablet of specified strength under the effect of compaction pressure.

Tableability is a key property for a given tablet press, but generally depends on equipment parameters such as punch velocity and is not scale independent. Compressibility is the ability of a

volume to undergo a reduction as a result of an applied force and has been described by numerous equations including those of Heckel [38], Kawakita [39], Adams [40] and Gurnham [41]. Tye et al. [33] showed the importance of tableting speed for some materials which show much poorer compressibility at high compression speeds. Patel et al. [2] highlighted the importance of material properties and tableting speed on the tableability, compressibility and compactibility of materials. In particular, the flowability and compaction challenges associated with direct compression for a poorly performing API at high loads were emphasised. Sun et al. [32, 42-44] considered formulation design of a high load tablet formulation. Flowability was considered by performing shear testing with blends of the API and different excipients with flow properties of MCC PH102 used as a threshold of acceptable flow. Plots of tableability of the various blends based on compactions on a simulator were used to rank compaction performance. A minimum tensile strength of 2 MPa was used to evaluate successful tablets. It was shown that key responses in high speed tableting, such as tablet weight variability, correlated with the shear measurements. Further work [43] showed that the reproducibility of flow properties of MCC PH102 from the different batches and manufacturers considered was sufficient to use it as a reference. The flow function of MCC PH102 was used in a recent study to evaluate the upper loading limit at which various APIs mixed with excipients are feasible for direct compression [44]. Pitt et al. [45] compare tableting behaviour between a small-scale benchtop press (Gamlen Tableting, United Kingdom) and a commercial scale Fette rotary tablet press (Fette, Germany). Two different formulations were considered, one DC blend and one WG blend. Tablets of different masses and shapes were considered with tensile strengths calculated according to the formulas in reference [46]. Predictions of compactibility, tableability, compressibility and ejection stress were all in agreement between the lab-scale and production presses, despite the differences in scale and equipment. The difference in tableting speed was not indicated, but, at least for the materials considered, did not influence results significantly. Ejection stresses on a small scale were shown to predict tablet failure at manufacturing scale for these products. Recent work by Osamura et al. [47, 48] also used a bench top tablet press (Gamlen Tablet Press (GTP-1)) with flat faced tooling to investigate formulation design for DC blends [39] and WG granules [40]. Formulations were assessed based on tensile strength, ejection stress and elastic recovery. Formulations with acceptable lab scale performance were shown to tablet well at a production scale on a rotary tablet press with oval shaped tablets. Low tensile strengths were observed to be indicative of tablet capping, while high ejection stresses were indicative of tablet binding to tooling. Such studies indicate that a scientific approach to lab scale testing of flow and compaction behaviour can be a very useful and efficient way to determine the feasibility and optimum formulation for a DC process, before conducting tests in a larger scale with selected

formulations. However, most studies to date do not consider a comprehensive range of excipient choices. Often, only one of flow or compaction behaviour is considered in detail and the optimal combination of these two bulk powder properties is not fully considered. Most studies use excipient blends only.

135 In this work, we present a new systematic design strategy to develop a formulation suitable for a continuous direct compression framework within a specified design space. The objective is to develop a design methodology which is rapid, material sparing, robust and allows accumulated knowledge to be transferred to other design problems. The methodology is tested using a case study on an industry posed formulation design problem with a difficult to process API, Canagliflozin, at a
140 high loading of 51 wt%. The strategy begins with a defined design space of allowable formulations and specified acceptable flow properties and critical quality attributes (CQAs) that the selected formulation should meet. Typically, the following information will be specified:

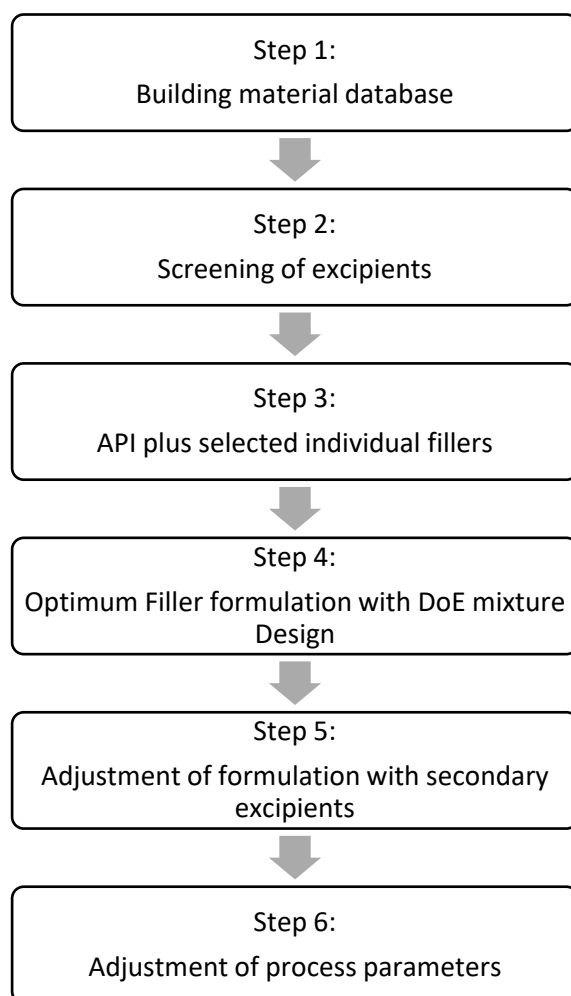
- API loading (wt%).
- The allowable wt% ranges given for lubricant, flow enhancer and disintegrant.
- 145 • Set of candidate fillers.
- Target flow properties and CQAs.

The strategy was developed by identifying a reduced set of key critical material attributes (CMAs) and critical process parameters (CPPs) which influence the CQAs. This was accomplished by
150 literature survey and the authors' experience. The formulation design space is iteratively reduced through careful screening of materials for favourable properties and accumulation of knowledge on how the CMAs of the screened materials and the process CPPs determine the final product CQAs. In this approach, excipient cost was not considered, as the focus was primarily on formulation and process design. The strategy presented here is illustrated graphically in Fig. 1 in section 2.1.

155

2 Materials and Methods

2.1 Formulation design strategy



160 *Fig. 1. Systematic formulation and process development for continuous direct compression.*

Building material database

Step 1 involves building a material database to investigate and understand the flow and compaction behaviour of the API and the set of possible excipients. Candidate materials are categorised into the functional classes used in this study (API, filler, lubricant, flow enhancer or disintegrant). The API loading is specified at 51 wt%. Fillers are added to improve the tablet properties such as tensile strength and dissolution behaviour. Flow enhancers are added in small quantities to improve the flowability of the formulation, a key requirement for continuous manufacturing processes. A small amount of lubricant is necessary to reduce friction with the tooling during compaction. The addition of disintegrants is considered for materials which fail to disintegrate in the desired time. The

candidate materials are extensively characterised using a suite of test methods to identify their physio-chemical properties and bulk flow and compaction behaviour as described in section 2.3. This process delivers quantitative, reproducible information on candidate materials and may be reused in future formulation designs.

175

Screening of excipients

Following material characterisation, step 2 is the screening of candidate excipients based on key performance indicators. Initial screening is based on flowability and tensile strength of tableted powders at a set pressure. Flowability measurements were performed on a powder rheometer (FT4, Freeman technology). The shear cell and compressibility % methodologies used are described in section 2.3.3. The compressibility test on the FT4 (CP%) is used as the primary flow indicator. This indicates the ability of a material to flow from an unpacked state. A secondary flow ranking is performed using the flow function from shear testing. This indicates the powders ability to flow from a pre-stressed (consolidated state). The flow function has been shown to be useful for ranking of flow behaviour from hoppers and tablet weight variability for high speed tableting [42, 44]. To ensure performance of selected powders throughout the process, only powders which pass requirements on both tests should be selected. Bivariate plots are used as a quick visual aid to rank powders based on flowability and tensile strength. Secondary ranking is performed based on disintegration behaviour. Excipients are not excluded on this basis if they rank well otherwise. Poor disintegration performance indicates the need for an excipient mixture or the inclusion of a disintegrant.

180
185
190

API performance with single fillers

Screened fillers are mixed with the API at the specified load to consider a set of possible formulations with a single filler (step 3). The flow, compaction and disintegration behaviour of the candidate blends are analysed as in step 2. Based on this, the design space is reduced to three selected fillers.

195

API performance with multiple fillers (Mixture DoEs)

Screened fillers may each exhibit strong performance in different areas (step 4). To ensure optimal blend performance ternary mixtures of the primary excipients with the API at the fixed load are considered. In order to minimise the number of experiments required to characterise the blend performance, a mixture design of experiments (DoE) is used to explore the design space. The characterisations in step 2 are repeated. At this stage, further experimental responses, which are

200

205 indicative of manufacturing performance, are added to allow more extensive ranking. These include mean yield pressure, tablet elastic recovery and tablet ejection stress. Based on this, two candidate blends are selected.

Formulation optimisation using secondary excipients

210 If required, the performance of selected blends may be further improved through the addition of secondary excipients (step 5). The level of flow enhancer may be varied within the allowable limits to improve the flow characteristics of the blends, while ensuring that it does not negatively impact tablet CQAs. If disintegration behaviour is an issue, the level of disintegrant may be varied within the selected limits. Secondary excipients should only be used when needed as they may have a negative
215 impact on tablet CQAs [47].

Scale-up of blends and adjustment of process parameters

Steps 1-5 are designed to limit the amount of trial runs on equipment so that time and material is spared. Following these steps, only the most feasible blends reach the scale-up and optimisation of
220 equipment parameters stage (step 6). The selected blends are rigorously assessed using the compaction triangle methodology on a lab-scale. The compactibility relationship has been shown by various authors to be scalable to high speed compaction and transferrable between equipment. Thus, it is used to set optimum target porosity and acceptable limits to reach the required tensile strength. Measures indicative of manufacturing issues, such as ejection and detachment stress and
225 elastic recovery, are considered in the target porosity range. Dissolution behaviour is also considered as a function of tablet porosity. Up to this stage, all tableting characterisations may be performed on a bench top compaction simulator at slow tableting speeds (punch velocity 1 mm s^{-1}) to minimise material used and ensure equipment measurement errors associated with dynamic tableting at high speeds are minimal. Once lab scale characterisation is completed, the influence of tableting speed
230 may be assessed using an instrumented rotary tablet press. The rate of compaction (punch speed) is most critical factor in the scale-up of tableting processes and most scale-up problems are speed related [41]. A batch run is performed to assess tablet weight variability and assess tablet CQAs to determine the success of the approach.

235 2.2 Materials

Canagliflozin (supplied directly by Janssen) was chosen as a model API. The formulation required a fixed load of 51 wt%. The remainder of the blend composition was made up of 0.5 wt% magnesium stearate as lubricant (Sigma-Aldrich), fumed silicone dioxide (Aerosil 200 Pharma, Evonik) as flow

enhancer (0 – 1 wt%) and a filler or a combination of fillers. Microcrystalline cellulose (MCC), calcium
 240 hydrogen phosphate (DCP), polyvinylpoly-pyrrolidone (PVPP), hydroxypropyl cellulose (HPC) and
 hydroxypropyl methylcellulose (HPMC) were used as fillers. Different grades of these were screened,
 which mainly differed in particle size distribution as specified in Table 1.

Table 1 List of filler materials included in formulation assessment.

Type of filler	Grade	Abbreviation	Vendor
Microcrystalline cellulose (MCC)	PH 101	MCC 101	Sanaq
	PH 102	MCC 102	Sanaq
Dicalcium phosphate(DCP)	Calcium hydrogen phosphate dihydrate	DCPD	Aliphos
	Kollidon® CL	KollCL	BASF
Crospovidone (PVPP)	Kollidon® CL-F	KollCLF	BASF
	Kollidon® CL-M	KollCLM	BASF
Hydroxypropyl cellulose (HPC)	L-HPC LH-11	HPC11	Shin-Etsu
	L-HPC LH-21	HPC21	Shin-Etsu
	L-HPC LH-31	HPC31	Shin-Etsu
Hydroxypropyl methylcellulose (HPMC)	Metolose® 60 SH - 4000	Met604000	Methocel E15 LV, Dow
	Metolose® 60 SH - 10000	Met6010000	Methocel E15 LV, Dow
	Metolose® 65 SH - 50	Met6550	Methocel E15 LV, Dow
	Metolose® 65 SH - 400	Met65400	Methocel E15 LV, Dow
	Metolose® 90 SH - 100 SR	Met90100	Methocel E15 LV, Dow
	Metolose® 90 SH - 4000	Met904000	Methocel E15 LV, Dow
	Metolose® 90 SH - SM 4000	Met90SM4000	Methocel E15 LV, Dow
	Metolose® 90 SH - 15000 SR	Met9015000	Methocel E15 LV, Dow
	Metolose® 90 SH - 100000 SR	Met90100000	Methocel E15 LV, Dow

2.3 Methods

2.3.1 Blend preparation

All small batch blends were prepared using a Caleva mini mixer at 60 rpm. The blends were prepared in following order: canagliflozin was pre-blended with silicon dioxide for three minutes (when used).

250 The filler(s) were added and mixed for further three minutes. Magnesium stearate was added last and mixed for just one minute to avoid it fully coating the particles [49]. For larger amounts of blends (> 25 g), a tumble mixer (Stuart STR4/3) at a rotation speed of 30 rpm was used. The material was added into a two-litre container with a maximum fill level of 50 % to ensure adequate mixing. The powders were added in the same order and using the same mixing times.

2.3.2 Raw material characterisation

Particle size distribution

The particle size distribution was determined using a laser diffraction analyser (Microtrac S3500).

The sample tray was filled up to one third (2 – 10 g) with the selected material and the analysis

method for irregular particle shape was used.

Density

Bulk density

The bulk density of all powders and blends was obtained from the powder compressibility test on the FT4 powder rheometer as outlined in section 2.2.3.

True density of pure components and blends

The true density (ρ_T) of the individual powders was determined using gas pycnometry (AccuPyc II 1340, Micromeritics) in a helium atmosphere. The true density of blends was determined according to the mass fraction x_i and true density ρ_{Ti} of each constituent powder. For an n-component blend the blend true density ρ_{Tb} is given by equation 1:

$$\frac{1}{\rho_{Tb}} = \frac{x_1}{\rho_{T1}} + \frac{x_2}{\rho_{T2}} + \dots + \frac{x_n}{\rho_{Tn}} \quad (1)$$

2.3.3 Powder flowability (FT4)

Compressibility test

The compressibility test is a standard test on the FT4 powder rheometer which measures the

percentage volume change of a powder under a set pressure of 15 kPa. The powder sample was

carefully pre-conditioned to ensure test reproducibility with a helical blade, which moved down and

up through the powder bed at a tip speed of 60 mm s⁻¹. After this step, the sample was split to

obtain a volume of 10 mL. The powder bed was slowly compressed with a vented piston to 15 kPa.

The change of powder volume was measured and the compressibility percentage (CP%) was

calculated using equation 2, where V_i was the initial powder volume and V_p the post compression

volume.

$$CP\% = 100 \times \frac{V_i - V_p}{V_i} \quad (2)$$

This test is similar to the compressibility index (Carr's index) calculated from the bulk and tapped powder density. In the absence of a specific benchmark for CP%, the USP flow characterisations for

Carr's index were adopted for the CP% here (Table S1, supplementary information). An upper limit of 20 % was chosen as this is the USP upper limit for "fair" flow (USP29 <1174> Powder Flow)[50].

Shear cell test

The flow function (FF) was determined using the standardised rotational shear cell test of the FT4 powder rheometer. The test was performed as described by Wang et al. [11], but only one pre-consolidation pressure of 9 kPa was used. The flow function after Jenike, which is a commonly used term for classifying flow behaviour of powders, is the ratio of the major principal stress (MPS) to the unconfined yield strength (UYS) as shown in equation 3. The classification of the flow type is listed in table S2 in the supplementary information.

$$FF = \frac{MPS}{UYS} \quad (3)$$

2.3.4 Tableting

Gamlen - benchtop compaction simulator

Compaction analysis was performed using a compaction simulator (Gamlen Tableting D series) using a 6 mm round and flat-faced punch and die set. The compaction was force controlled with loads of 50 – 500 kg applied at a controlled upper punch velocity of 1 mm s⁻¹. For each compression 100 mg of sample was manually filled into the die and compacted. The load-displacement data was used to perform in-die Heckel analysis and calculate detachment and ejection stresses. Punch elastic deformation was incorporated into the calculations. To determine the punch deformation, a compaction with an empty die was performed.

Piccola – R&D rotary tablet press

Scale-up to a multi-station system was performed on a ten station turret R&D Riva Piccola rotary tablet press equipped with eight round, flat-faced 8 mm punch and die sets. Two of the ten stations were blanked. The target OSD weight was 200 mg. The turret speed could be adjusted from setting 1 to 10 (~2 – 50 rpm), allowing a maximum tablet output of 30,000 tabs h⁻¹. The compaction load range could be adjusted from 1 – 60 kN on the main compaction roll. The blend was gravity fed via a hopper. For all tests, the pre-compaction force was set to zero. The raw data was exported to excel giving dwell, contact, rise, fall and pulse time and forces of the individual punches during compression and ejection.

Compaction and tablet characterisation

Tensile strength

315 The tablet crushing force (hardness) F was determined using a diametrical compression test. For
OSDs compacted on the Gamlen triplicates for each compaction condition were tested for hardness
using a PTB 311E, Pharma Test hardness tester. This equipment also records the tablet diameter D
and thickness h . OSDs compacted on the Piccola were characterised using a semi-automated tablet
testing system (SmartTest 50, Pharmatron Dr. Schleuniger®). The SmartTest 50 records tablet weight
320 w , diametrical crushing force F , tablet diameter D and thickness h . As larger amounts of OSDs were
available, 10 tablets per condition were tested for hardness and 30 in total for dimensions and
weight. The tablet tensile strength (cylindrical tablets) was evaluated using equation 4 [51]:

$$\sigma_t = \frac{2 F}{\pi D h} \quad (4)$$

Tensile strength values typically range from 0.1 – 4 MPa, while values in excess of 1 MPa are usually
desirable for tablets [24]. Pitt et al. [45, 46] recommend tensile strengths in excess of 2 MPa to
325 ensure a satisfactorily robust product.

Tablet porosity and relative density

The porosity of a tablet ε can be calculated during compaction (in-die), since the punch
displacements are recorded, and after compaction (out-of-die) by measuring the tablet dimensions.
The tablet porosity is given by

$$\varepsilon = 1 - \frac{\rho_{app}}{\rho_T} = 1 - \frac{4 m}{\rho_T \pi D^2 h} \quad (5)$$

330 where m is the tablet mass, ρ_{app} is the apparent tablet density and ρ_T is the true density of the
powder or blend making up the tablet. The tablet porosity is related to the tablet solid fraction or
relative density γ by

$$\varepsilon = 1 - \gamma \quad (6)$$

Typically, solid fractions in the range 0.85 ± 0.05 are optimal for tablet formulations [45, 52]

Compaction pressure and load

335 Compaction pressures across the two devices ranged from 0 – 250 MPa covering the range of tablet
porosities of interest.

Elastic recovery (%)

340 The immediate axial elastic recovery percentage $\%ER_0$ and axial elastic recovery after approximately 48 hours $\%ER_{48}$ was measured and evaluated. Further information and equations S1 and S2 can be found in the supplementary material.

Ejection and detachment stresses

Force-displacement data was collected during the processes of tablet ejection and detachment from
345 the lower punch. Excessive forces during these stages can lead to, or indicate a risk of, production issues such as sticking, capping or lamination. The ejection stress ES is the maximum force F_E observed during ejection, divided by the tablet surface area in contact with the die walls [53, 45, 47]. For a cylindrical tablet it is given by

$$ES = \frac{F_E}{\pi D h} \quad (7)$$

For commercial requirements, an ejection stress less than 3 MPa generally suffices to produce a
350 tablet which does not cap or laminate and ejection stresses up to 5 MPa may be acceptable [45].

The detachment stress DS is calculated by dividing the maximum force observed during detachment F_D (sometimes referred to as the take-off force) by the area in contact with the lower punch. For a cylindrical tablet it is given by

$$DS = \frac{F_D}{\pi D^2} \quad (8)$$

The detachment stress may be higher or lower than the ejection stress depending on material
355 properties. Detachment stresses which are significantly higher than ejection stresses can be considered to indicate the risk of production issues [54]. These properties are dependent on the compaction pressure applied or the degree of compression and should be evaluated at an appropriate porosity.

Heckel analysis

360 Heckel analysis was performed to characterise the compressibility (pressure-porosity relationship) and the mean yield pressure P_y [49]. Further detailed information can be found in the supplementary material.

Compaction triangle

365 The compaction triangle was used to relate the key critical process parameters and critical quality attributes in the tableting process, namely the compaction pressure, the tablet porosity (or solid

fraction) and the tablet tensile strength. The equations chosen to relate these variables in this work are outlined below

Tabletability (tensile strength-compaction pressure) In this work, tabletability was described as a linear function of the maximum applied pressure [55, 56]:

$$\sigma_t = aP_{max} + b \quad (9)$$

where P_{max} is the maximum applied pressure and a and b are constants. The constant a is a parameter which quantifies the increase of the tensile strength per unit increase in the maximum applied pressure.

Compactibility (tensile strength-porosity) The Ryshkewitch-Duckworth equation [36, 37] was used in this study. It is defined as:

$$\sigma_t = \sigma_{t0}e^{-k\varepsilon} \quad (10)$$

where σ_{t0} is the tensile strength of a tablet at zero porosity, and k is a material constant representing the bonding capacity of the material [57].

Compressibility (porosity-compaction pressure) is evaluated out-of-die, by recording the dimensions of resulting tablets for different maximum applied pressures. Elastic recovery means the results differ from the in-die relationship. In this study, an exponential relationship between porosity and pressure was used (Heckel equation in exponential form):

$$\varepsilon = A^*e^{-KP} \quad (11)$$

where $A^* = e^{-A}$ relates the two forms of the equation.

Weight uniformity (Piccola)

Tablet weight variability was assessed by taking a random sample of tablets for each compression condition ($n = 20$) on the Piccola. The weight variability was assessed by considering the relative standard deviation of tablet weight (RSD). The relative standard deviation RSD is calculated by dividing the standard deviation of the sample s , by the sample mean tablet mass \bar{m} . The RSD was reported as a percentage given by

$$RSD = 100 \times \frac{s}{\bar{m}} \quad (12)$$

Disintegration

Disintegration was carried out in line with USP guidelines (USP <701>)[58]. A full description of the method is included in the supplementary material.

Dissolution

Dissolution studies were carried out with a USP compliant tablet dissolution apparatus type II (Pharma Test PTWS 120D). The testing conditions are outlined in Table S2 in the supplementary information. For sample analysis, high pressure liquid chromatography (HPLC, Agilent Technologies 1260 Infinity) was used. The actual API concentration was determined via a calibration curve, which was prepared pre-testing. The pass quality criterion required 80 % of the API to be dissolved by 20 minutes and 85 % at 30 minutes.

2.3.5 Statistical analysis

Design of experiments (DoE) and subsequent statistical analysis was performed with the Design Expert® 9 statistical software from Stat-Ease, Inc. Further data analysis was carried out using R (version 3.4.2) with integrated development environment RStudio (version 1.1.383).

Fitting of regression models and response surfaces is performed using standard techniques. Full details of the statistical techniques used are included in supplementary material.

3 Results and Discussion

3.1 Material database

In total 19 fillers, 4 APIs, 1 flow enhancer, 1 disintegrant and 2 lubricants were characterised. Particle size distribution, moisture content, true and bulk densities, compressibility percentage, cohesion, flow function and flow rate index were compiled in the database (supplementary information table S4). The tableting behaviour of each powder was assessed and tablet properties such as disintegration behaviour, tensile strength and porosity under set conditions were also determined.

3.2 Screening of excipients

Compressibility percent (CP%) was used as the key flow indicator. Tensile strength was selected as the critical tablet property, along with disintegration ability as a secondary response. Fig. 2 categorises material suitability for continuous direct compression. Ideally, the final blend should be in quadrant I, where the selected limits of tensile strength greater than 2 MPa and a CP% less than 20, are both satisfied. Canagliflozin (Cana) sits in quadrant IV representing poor flow and poor tensile strength. Quadrant II represents the ability of forming strong tablets, but poor flowability. However, poor flow may be improved with flow enhancers and/or a combination of various fillers. Quadrant III shows materials with good flowability, but requiring higher pressures to form strong compacts.

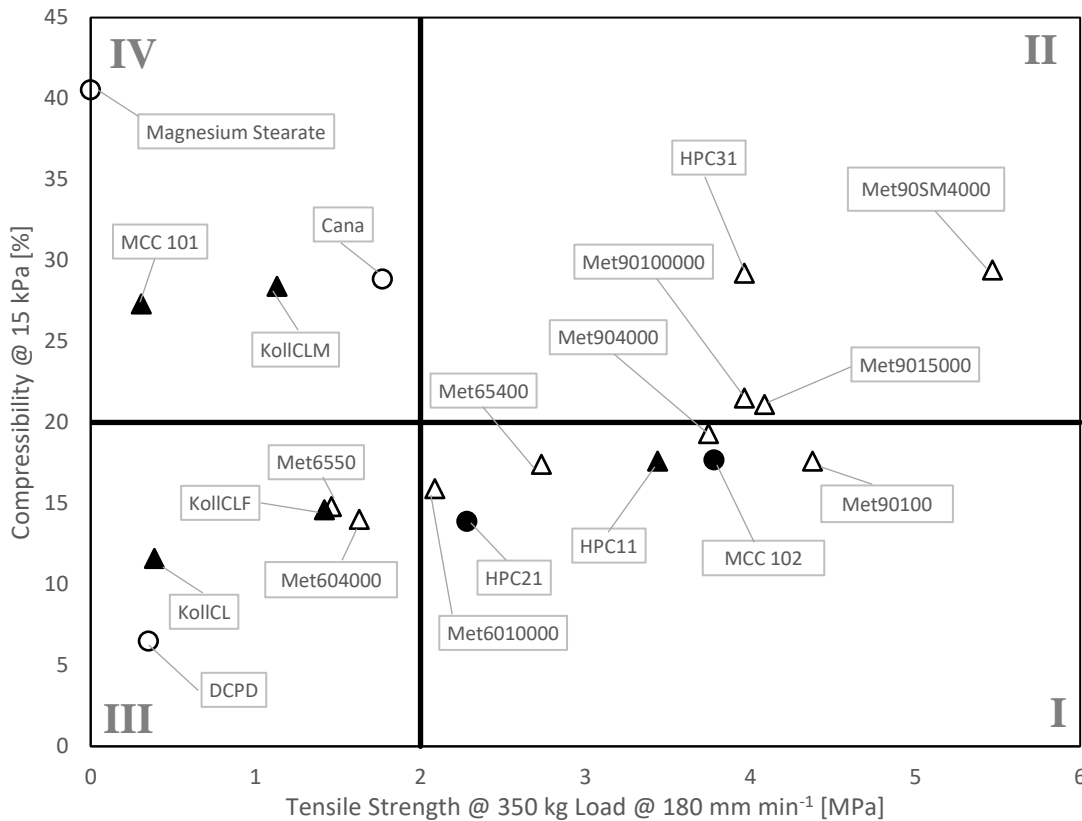


Fig. 2. Screening and categorising materials for flow and compaction behaviour. Quadrant I and III indicate good flowability; quadrant I and II indicate good compaction properties in terms of tensile strength. All materials with open symbols indicate that no disintegration occurred. The materials with open or filled circles were selected for further evaluation.

The selected fillers were initially ranked by their flow and compaction behaviour as outlined in the methods section. Secondary responses of disintegration and electrostatic charging were also evaluated. Table 2 shows the best representative of each of the five fillers chosen based on the initial screening. Electrostatic charging (e^- charging) was evaluated visually during flowability testing, where some materials heavily adhered to the tooling while stirring. The filler suitability was determined based on a combination of responses including electrostatic charging, flow behaviour, disintegration and tablet tensile strength. The key responses were flowability and tensile strength. Flow behaviour was evaluated using the FF and CP% tests and ranked based on the flow evaluation tables S1 and S2 in the supplementary material. Free flowing powders are indicated with '+', slightly cohesive to free flowing with '0' and cohesive with '-'. A disintegration time under 5 minutes was classified as '+', between 5 and 15 as '0' and over 15 minutes as '-'. A good tensile strength was defined as above 2 MPa, whereby a poor tensile strength was considered below 1 MPa. The best performing representative grade of each material group was chosen, namely MCC PH 102, DCPD,

Kollidon® CL (PVPP), L-HPC-LH21 and Metolose® 60 SH – 4000 (HPMC). From all materials screened, these materials indicated the best filler suitability in terms of flowability and tensile strength.

445

Table 2 List of pre-selected filler materials. Materials are ranked on required properties for a continuous direct compression process. Performance is ranked as good (+), medium (0) or poor (-).

	Flow behaviour	e ⁻ charging	Disintegration	Tensile Strength	Filler suitability for DC
MCC 102	0	+	+	+	+
DCPD	+	+	-	0	0
KollCL (PVPP)	+	+	+	0	+
HPC21	+	+	0	+	+
Met604000 (HPMC)	+/-0*	+	-	0	0

*FF = +, CP% = 0

450 3.3 API with single (screened) fillers

Single filler blends with a 51 wt% API loading were prepared using the five selected fillers.

Canagliflozin is a hemi-hydrate so 51 wt% was given as a fixed requirement for this application to achieve 50 wt% API dosage. No other excipients except the filler was added. These blends were fully studied to evaluate their flow and compaction responses relative to the API powder alone. Fig. 3

455 shows the CP% vs. tensile strength plot including the individual materials and the blends (bold). The open symbols indicate that no disintegration took place. The FF was also determined to ensure that at least two measures were taken to evaluate flowability. The FF (not shown in graph) indicated

similar flow behaviour as the CP%. The addition of any filler, except for Kollidon® CL, showed significant improvement in flowability and a stable or increased tensile strength. Due to the lack of

460 disintegration, dissolution was only carried out for the blends containing MCC PH 102, L-HPC-LH21 and Kollidon® CL. (Fig. 4). All three blends passed the requirements for dissolution and matched or

had a higher initial dissolution rate than the reference dissolution profile from the current wet-granulated formulation, which is indicated by the dashed reference profile. The slight variations of the final API concentration from 100 % is due to slightly lower or higher actual API concentration

465 than targeted. This could be due to incomplete mixing of the blends. The five fillers were narrowed down to three, specifically MCC PH 102, L-HPC-LH21 and DCPD. Kollidon® CL was excluded due to its negative impact on both flow and tensile strength responses. Metolose® 60SH 4000 was excluded because, even with the aid of disintegrants, the tablets would not disintegrate. Instead the tablets swelled, which is a common attribute of this material. As for this specific API a fast disintegration

470 was desired, it was excluded from further studies as made it unsuitable for the current formulation development. However, due to its good compaction and flow behaviour it is a potential candidate

for direct compression. Although DCPD did not disintegrate, it was chosen due to its excellent flow properties. Through initial trials it was established that disintegration would take place once a disintegrant, or a filler which acts as a disintegrant, was added.

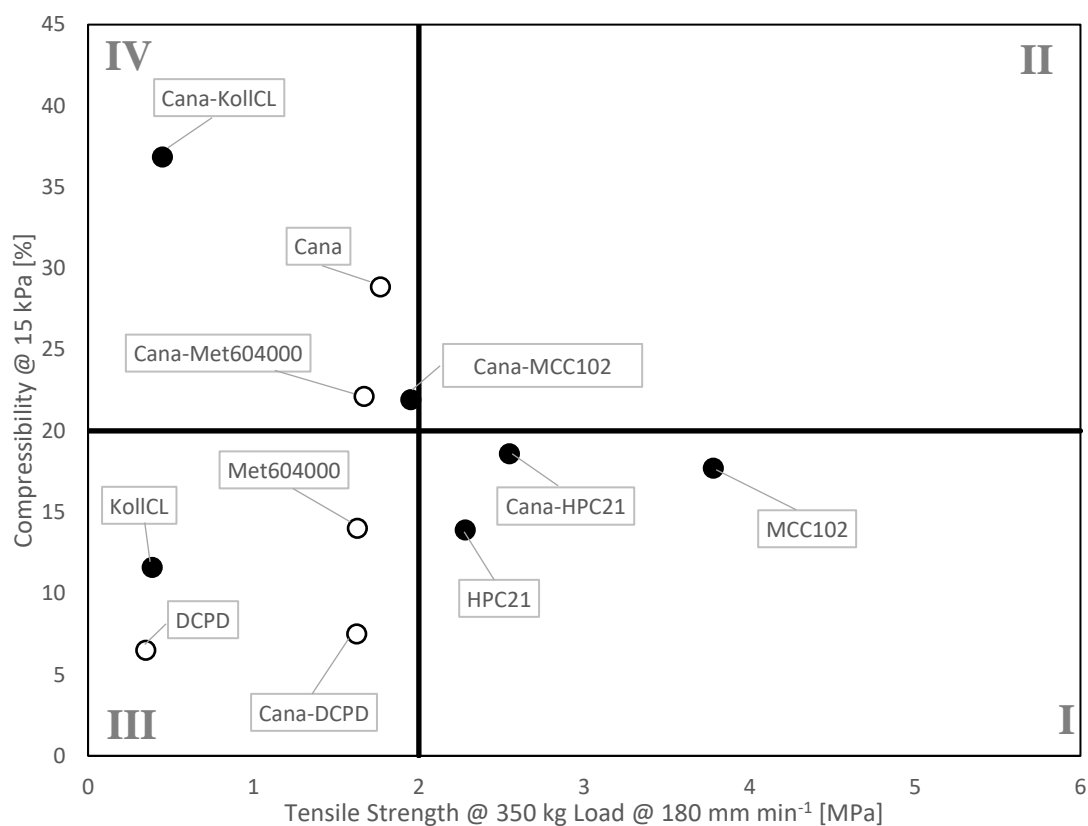


Fig. 3. Evaluation of single filler blends via compressibility, tensile strength and disintegration behaviour. Open symbols indicate that no disintegration took place.

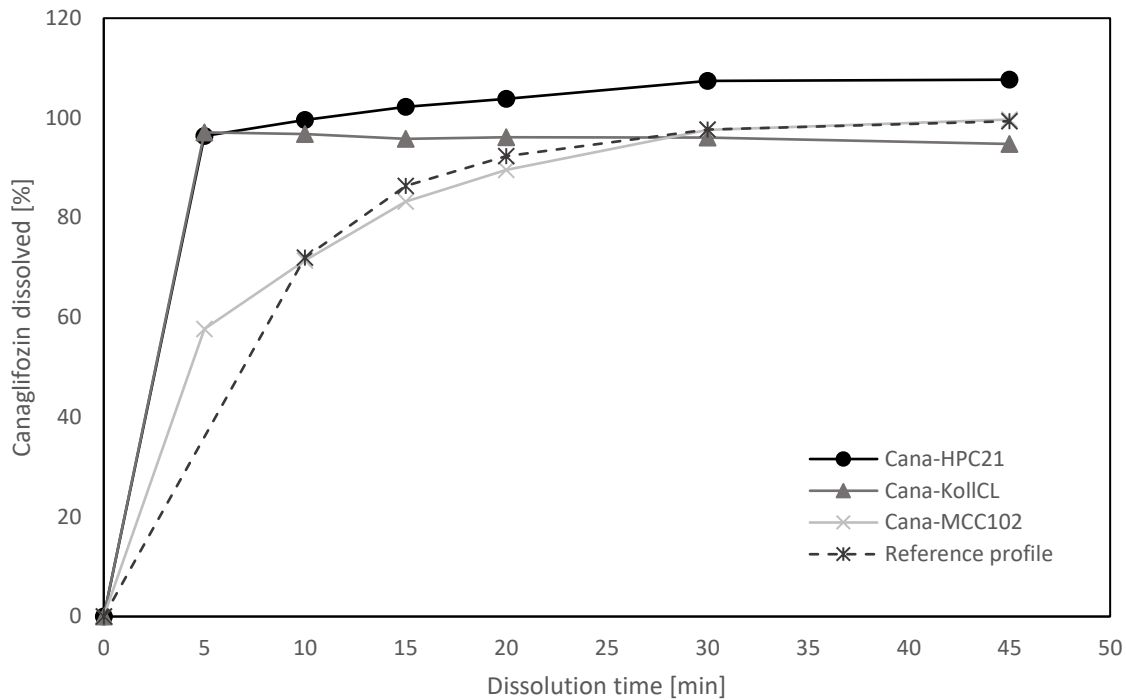


Fig. 4. Dissolution plots of the single filler blends. The blends containing DCPD and Metolose® 60 SH 4000 were not included since no disintegration took place.

3.4 Mixture DoE to optimise blend

The filler portion of the formulation can be made up of mixtures of different filler materials to maximise the performance of the formulation. A mixture design of experiments (DoE) was carried out in order to find the combination of the three selected fillers which would optimise the flow and compaction properties of the formulation. A simplex lattice design with three levels comprising 10 runs was chosen (Fig. 5). The blends all consisted of 51 wt% canagliflozin and 0.5 wt% magnesium stearate. The loadings of MCC PH 102 (MCC), L-HPC-LH21 (HPC) and DCPD (DCP) were varied according to the design between 0 and 48.5 wt%. The filler composition of the individual runs is listed in Table 3. All blends were prepared in the Caleva mini mixer (20 g) and later compacted in triplicates using the Gamlen compaction simulator at 350 kg load and 100 mg unit sample.

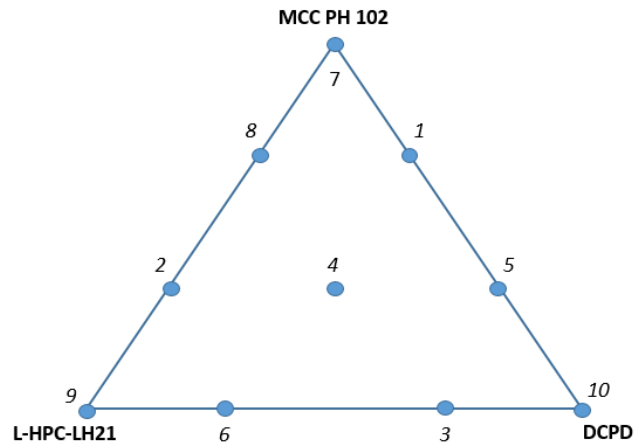


Fig. 5. Mixture design, simplex lattice with three levels. Each of the numbered points represents a blend with varying concentration of fillers. The API loading of 51 wt% and lubricant concentration (MgSt) at 0.5 wt% was set constant.

The key responses listed in Table 3 were the FF, CP%, conditioned bulk density (CBD), tensile strength (σ_t), disintegration time (D_t), porosity (ε), mean yield pressure (P_y), immediate elastic recovery (ER_0) and elastic recovery after 48 hours (ER_{48}), along with the measured blend particle size distributions (d_{10} , d_{50} , d_{90}).

Table 3 Overview of the mixture design and measured blend properties and responses.

Run #	MCC [wt%]	HPC [wt%]	DCP [wt%]	FF [-]	CP% [%]	CBD [g cm ⁻³]	σ_t [MPa]	D _t [s]	ε [-]	P_y [MPa]	ER ₀ [%]	ER ₄₈ [%]	d ₁₀ [μm]	d ₅₀ [μm]	d ₉₀ [μm]
1	32.3	0	16.2	8.2	17.1	0.484	2.25	23	0.12	45.86	9.5	13.6	12.74	46.8	204.8
2	16.2	32.3	0	6.3	18.8	0.440	2.85	18	0.12	40.80	8.7	14.9	11.81	42.73	151.9
3	0	16.2	32.3	11.0	14.3	0.570	2.18	8	0.14	51.02	9.6	14.3	10.05	38.97	96.19
4	16.2	16.2	16.2	9.0	16.6	0.498	2.35	70	0.14	56.93	9.0	12.5	11.76	42.38	151.7
5	16.2	0	32.3	10.8	13.7	0.555	1.99	12	0.16	61.56	9.8	12.8	8.97	39.86	147.1
6	0	32.3	16.2	9.5	14	0.531	2.53	15	0.14	55.13	8.8	12.6	7.29	36.86	95.12
7	48.5	0	0	9.7	22	0.406	2.51	40	0.13	51.86	8.6	11.8	11.74	47.77	216.8
8	32.3	16.2	0	7.7	22.1	0.422	2.58	12	0.12	49.50	8.8	11.6	10.96	44.65	195
9	0	48.5	0	3.2	17.9	0.450	2.62	21	0.12	44.50	8.4	12.3	8.22	38.25	94.59
10	0	0	48.5	19.5	11	0.650	1.86	-	0.15	79.28	10.0	9.2	7.71	36.16	95.53

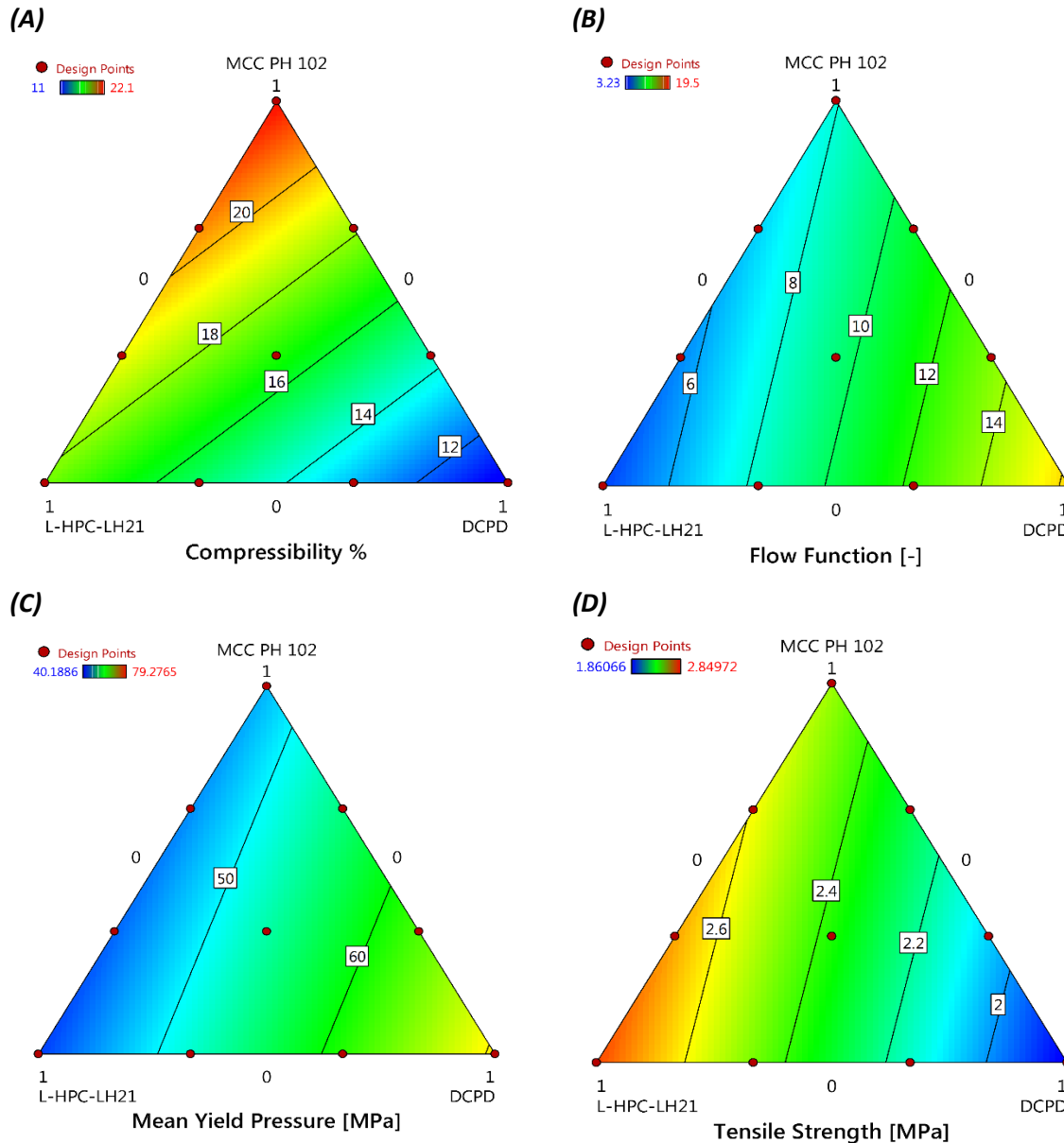
505 Collected data was plotted and analysed. The behaviour of responses based on filler composition was captured using data driven models. The predictive power of different models was assessed. Contour plots of selected responses on ternary diagrams are shown in Fig. 6. Each point in the diagram corresponds to a given mixture of the three excipients in question. The excipient wt% range of 0 - 48.5 wt% has been normalised to 0 - 1. The sum of the excipient amounts used must equal
510 unity. The triangle's vertices represent the use of single components as excipients. The edge opposite a vertex represents zero wt% of the component at that vertex. The wt% of that component increases linearly from zero to one along the line connecting the centre point of the edge to the opposite vertex. Thus, points on an edge are mixtures of two components and points in the interior of the triangle cover mixtures of the three components in all proportions, where all components are
515 non-zero. The contour map corresponds to the response level. The models listed in Table 4 were obtained by model reduction to their significant effects and show a p-value under 0.05 for the F-test for model significance, indicating a statistically significant fit. The two responses for flowability, which are CP% (Fig. 6 (A)) and the FF (Fig. 6 (B)), both indicate reasonable fits to the existing data when looking at the R^2 and adjusted R^2 . However, based on the predicted R^2 value for this data, only
520 CP% could be considered accurate for prediction within the design space. Therefore, CP% was chosen as the main predictor for flowability. Both FF and CP% confirm that blends containing DCPD give the best flowability. However, FF and CP% give opposite rankings for the L-HPC-LH21 and MCC PH 102 blends. The FF indicates poor flowability for HPC and fair flowability for MCC, whereby CP% indicates good flowability for HPC and fair flowability for the MCC blend. The bulk density was also
525 recorded, and similarly to the CP%, is highly predictable.

In order to assess the tableting performance, Heckel analysis was carried out and the mean yield pressure σ_t was determined (Fig. 6 (C)). The lower the mean yield pressure P_y , the less force is required to form a compact (see section 2.3.4 under Heckel analysis). The plot indicates that using L-HPC-LH21 as a single filler, has the lowest mean yield pressure (<50 MPa) closely followed by MCC.
530 High concentrations of DCPD, however, require significantly more pressure (~70 MPa) to form a compact. Mean yield pressure is also very predictable based on the mixture of components.

The tensile strength was identified as a key factor to assess the OSD characteristics and is shown in Fig. 6 (D). The tensile strength is very predictable and indicates that a high concentration of L-HPC-LH21 (~45 - 48.5 wt%) would produce OSDs at a desired tensile strength of over 2.6 MPa.
535 Similarly, MCC PH 102 produced a tensile strength over 2.4 MPa. In both cases, a desired porosity between 0.10 and 0.15 was attained. The formulations containing high amounts of DCPD (>30 wt%) indicated the lowest tensile strengths, with values under 2 MPa.

Table 4 Model overview of potential predictable responses with significant *p*-value.

	Model type	<i>p</i> -value	R^2	Adjusted R^2	Predicted R^2
(A) Compressibility %	linear	<0.0001	0.9326	0.9133	0.8814
(B) Flow function	linear	0.0044	0.7885	0.7281	0.4244
(C) Mean yield pressure	linear	0.0001	0.9279	0.9073	0.8463
(D) Tensile Strength	linear	0.0001	0.9211.	0.8385	0.7964
Bulk density	linear	< 0.0001	0.9916	0.9892	0.9814
Porosity	linear	0.0286	0.6378	0.5343	0.3360
Elastic Recovery 0 h	linear	0.0051	0.7787	0.7155	0.6000



540 Fig. 6. Contour plots of selected responses: (A) compressibility %, (B) flow function, (C) mean yield pressure and (D) tensile strength.

The optimum pre-formulation including the API and main filler was selected using the graphical optimisation tool in the Design Expert® software (Fig. 7). The limits for CP% (max. 18 %) and σ_t (min.

2.7 MPa) were chosen to select the region of minimum CP% and maximum tensile strength. These limits are marked in the figure. The intersection of these two regions gives the optimum formulation. Based on Fig. 7. the best choice is a formulation comprising 48.5 wt% L-HPC-LH21 as a single filler.

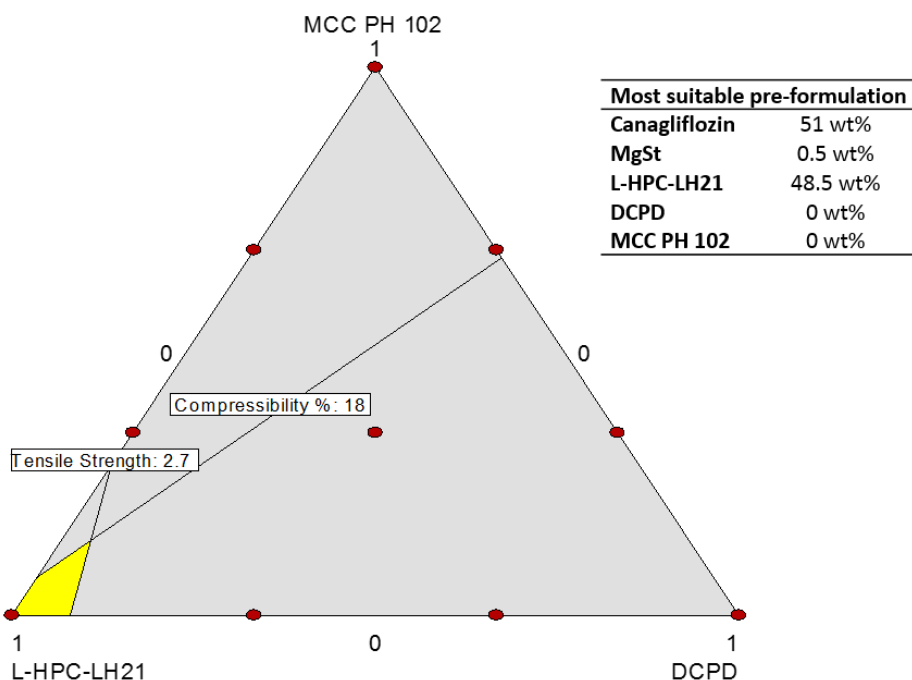


Fig. 7. Overlay plot of the tensile strength and CP% for establishing the most suitable pre-formulation. The limits were narrowed to a tensile strength of 2.7 MPa and a CP% of 18. The most suitable formulation is outlined in the table.

Dissolution was carried out for each of the 10 tableted blends. The dissolution profiles can be found in the supplementary material in Fig. S1, whereby the red dashed line is the reference profile (RP) which refers to the commercially used wet granulated formulation. Fig. 8 shows the canagliflozin dissolved (%) at time point 20 (grey bars) and at time point 30 (hatched bars) of the 10 DoE runs and the reference profile (RP). The dashed line indicates the 80 % pass criterion for the 20-minute time point and the dotted line indicates the 85 % pass criterion for the 30-minute time point. Three blends (run 1, 5 and 10) failed the pass criterion of having 80/85% of the API dissolved by 20/30 minutes. Those three blends are either a combination of only MCC PH 102 and DCPD or only DCPD. Provided L-HPC-LH21 is involved in the formulation with DCPD, the dissolution passes the criterion. The failure of the dissolution of DCPD as a single filler (run 10), was expected, as no disintegration took place in earlier tests. Interestingly, the disintegration time does not appear to be directly linked

with the dissolution performance; samples, which had a longer disintegration time could still perform faster in dissolution than samples which had a rapid disintegration time.

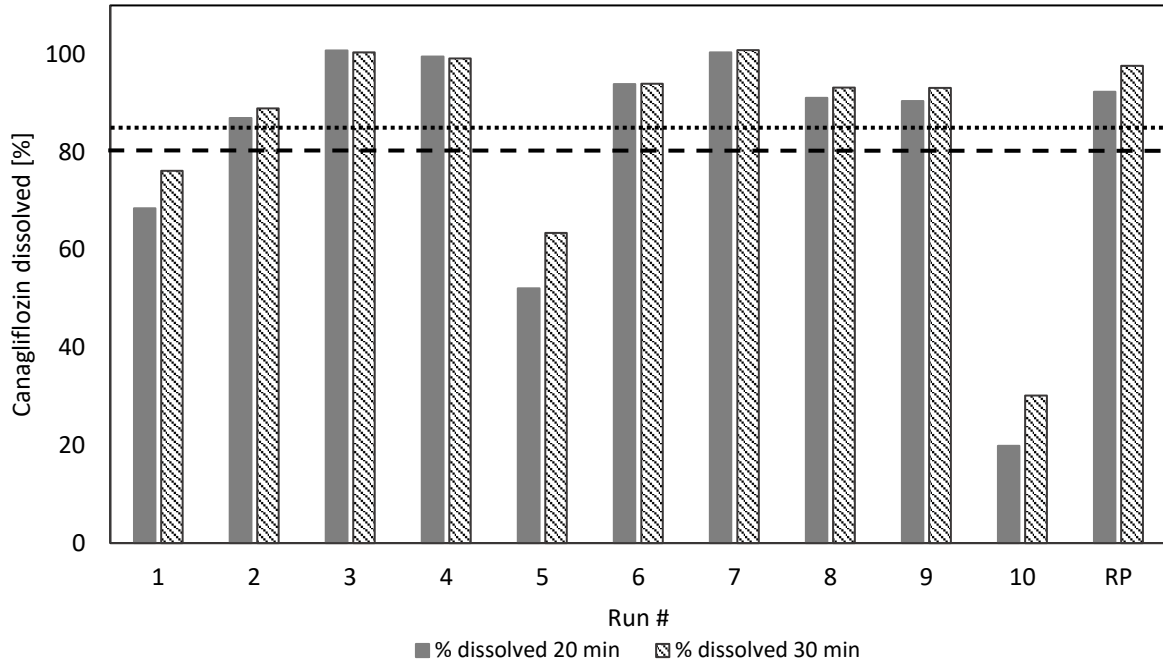


Fig. 8. Canagliflozin dissolved in % at time point 20 minutes (grey bars) and 30 minutes (hatched bars) of the 10 DoE runs listed in Table 3 and the wet granulated reference profile (RP). The dashed line indicates the 80 % pass criterion for 20 minutes and the dotted line the 85 % pass criterion for 30 minutes.

As the flowability can still be improved in the next step using a flow enhancer, the compaction behaviour was prioritised over flowability in this step. The mixture design showed that L-HPC-LH21 performed best as a single filler. However, due to its excellent dissolution behaviour and good compaction behaviour, the single filler MCC PH 102 blend was chosen as an alternative blend. The inclusion of a separate blend reduces the risk of failure and allows for further evaluation of the optimum formulation.

3.5 Adjustment of formulation using secondary excipients

580 The selected pre-formulations contain 51 wt% canagliflozin, 0.5 wt% magnesium stearate and 48.5 wt% of either L-HPC-LH21 or MCC PH 102. Both blends show good compaction behaviour, but improvements in flow behaviour are desirable. Therefore, varying amounts of Aerosil 200 (fumed silicon dioxide) were added as flow enhancer. The chosen levels were 0.2, 0.4 and 0.6 wt%. Canagliflozin was pre-blended with SiO₂ first to allow time for coating of the poor flowing API

585 particles. SiO₂ improves the flow in two ways. Firstly, SiO₂ are very small spherical particles and act as spacer between the bigger irregular shaped particles and improve particle packing to enhance the flow behaviour. Secondly, SiO₂ also changes the charge of the blend, reducing the overall electrostatic charges allowing the blend to flow more easily [59, 60]. However, too much or too little SiO₂ can lead to poorer flow behaviour and can impact tablet properties such as tensile strength, disintegration and dissolution [59, 61]. Fig. 9 outlines the effects of the various silicone dioxide levels. Fig. 9 (A) and (B) show the CP% and FF for investigating the flow behaviour. For the MCC blend, an SiO₂ concentration of 0.2 wt% indicates the best CP%. The FF does not show a significant difference between the varying SiO₂ levels. For the HPC blend the best CP% is achieved with 0.4 wt% SiO₂. The addition of SiO₂ increases the tensile strength to over 2 MPa and the disintegration time

595 for both formulations (Fig. S2 (A) and (B)). Both increases are most likely due to the better particle packing, which is reflected in the relative density (Fig. S2 (C)). In the dissolution profiles (Fig. S2 (D)), no significant changes were observed, and all passed the requirements. Due to the positive changes in tensile strength and relative density regardless of SiO₂ level, the focus was on selecting the blends with the best flow behaviour. Although the disintegration time increased marginally with the

600 addition of SiO₂, they were all still in an acceptable time range.

The selected adjusted formulations were:

- 51 wt % canagliflozin, 0.4 wt% SiO₂, 48.1 wt% HPC21, 0.5 wt% magnesium stearate.
- 51 wt % canagliflozin, 0.2 wt% SiO₂, 48.3 wt% MCC 102, 0.5 wt% magnesium stearate.

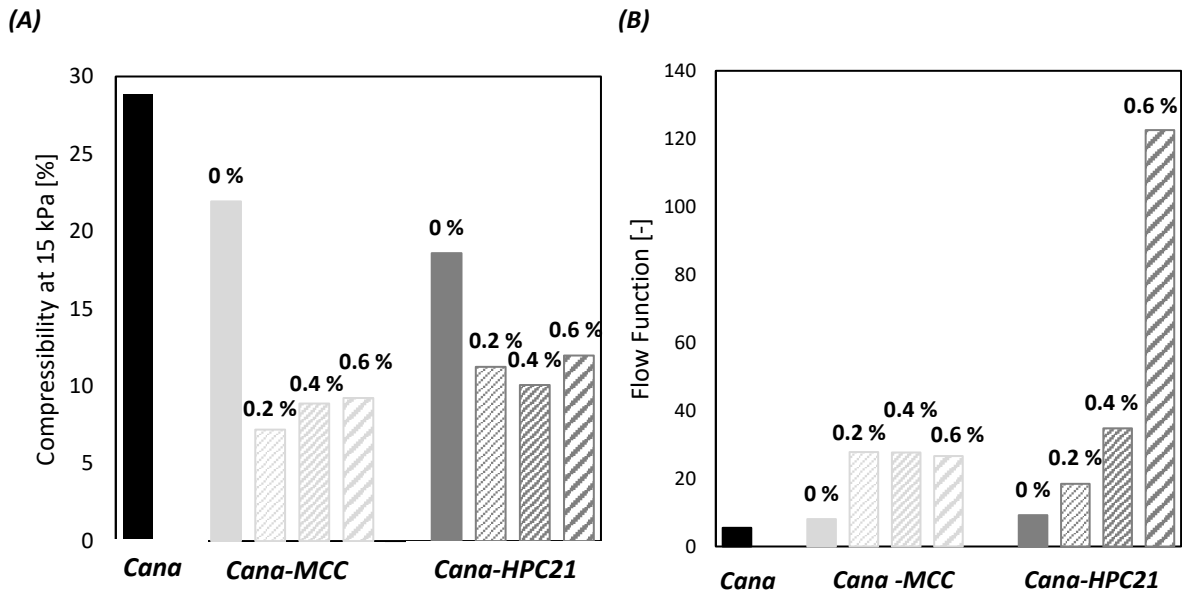


Fig. 9. Impact of silicone dioxide levels on compressibility % (A) and flow function (B). The percentages on the bars indicate the SiO₂ loading.

3.6 Adjustment of process parameters and scale-up of blends

The previous steps have been conducted in order to select the formulations most likely to succeed at manufacturing scale (e.g. 250000 – 50000 tablets per hour). To facilitate a rapid and successful scale-up of the selected formulations, their behaviour in response to key equipment operating parameters was then extensively characterised. In order to test the suitability of the two developed formulations for manufacturing scale, the following key responses were assessed:

- Ejection and detachment stresses under varying compaction pressures.
- Dissolution behaviour of formulations compacted under varying compaction pressures.
- Tableability, compressibility and compactibility of formulations on different equipment and tableting speeds.

The selection of compaction pressure, tableting speed and equipment together determine the tablet porosity, which is identified as a key CQA. To evaluate any tendency for capping or lamination in the chosen formulations, the tablet detachment stresses from the lower punch and tablet ejection stresses out of the die were measured for tablets compacted under six different pressures on the Gamlen, which led to different porosities (Fig. 10). Ejection and detachment stresses tend to be similar. A maximum ejection stress of 5 MPa has been specified as acceptable for the compaction speed on the Gamlen. The detachment stress should not be significantly larger [54]. If there was a risk of capping or lamination, small hair fractures and/or sticking may be observed. Fig. 10, shows that the ejection and detachment stresses for the HPC formulation remain very low until very low

porosities are reached ($\epsilon < 0.07$). In contrast, the MCC formulation shows significantly higher stresses at the porosities of interest for manufacturing. Despite this, both formulations pass on the basis of the 5 MPa cut-off point.

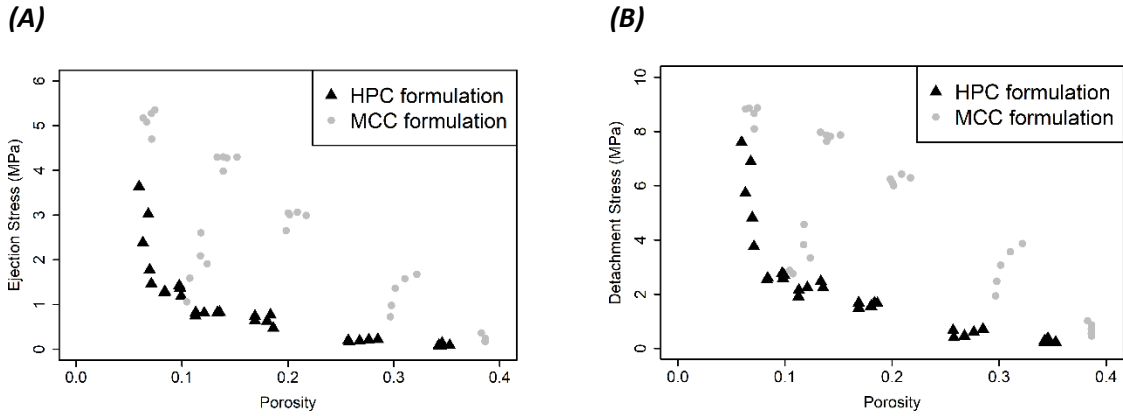


Fig. 10. Plots of ejection stress (A) and detachment stress (B) vs. porosity for both finalised MCC and HPC formulations. The ejection and detachment stresses remain very low for the HPC formulation until very low porosities are reached. The stresses for the MCC formulation increase more rapidly as porosity decreases, indicating a higher potential for lamination and capping issues during manufacturing.

Dissolution was carried out for each conditions (Fig. 11) noting the related porosities and compaction pressure in brackets. The darker the shade the higher the compaction pressure and lower the porosity. For both formulations, a decrease in the porosity resulted into a slower dissolution. However, both formulations at any of the prepared porosities fulfilled the formulation requirements. For the MCC blend a significant difference between the profiles can be seen (Fig. 11 (B) and (D)), which shows a significantly slower dissolution than HPC at lower porosities. While the tablets at intermediate scale are larger, their rapid disintegration time suggests similar dissolution profiles for similar porosities as seen in the dissolution profiles of the tablets produced on the Piccola (Fig. 11 (C) and (D)).

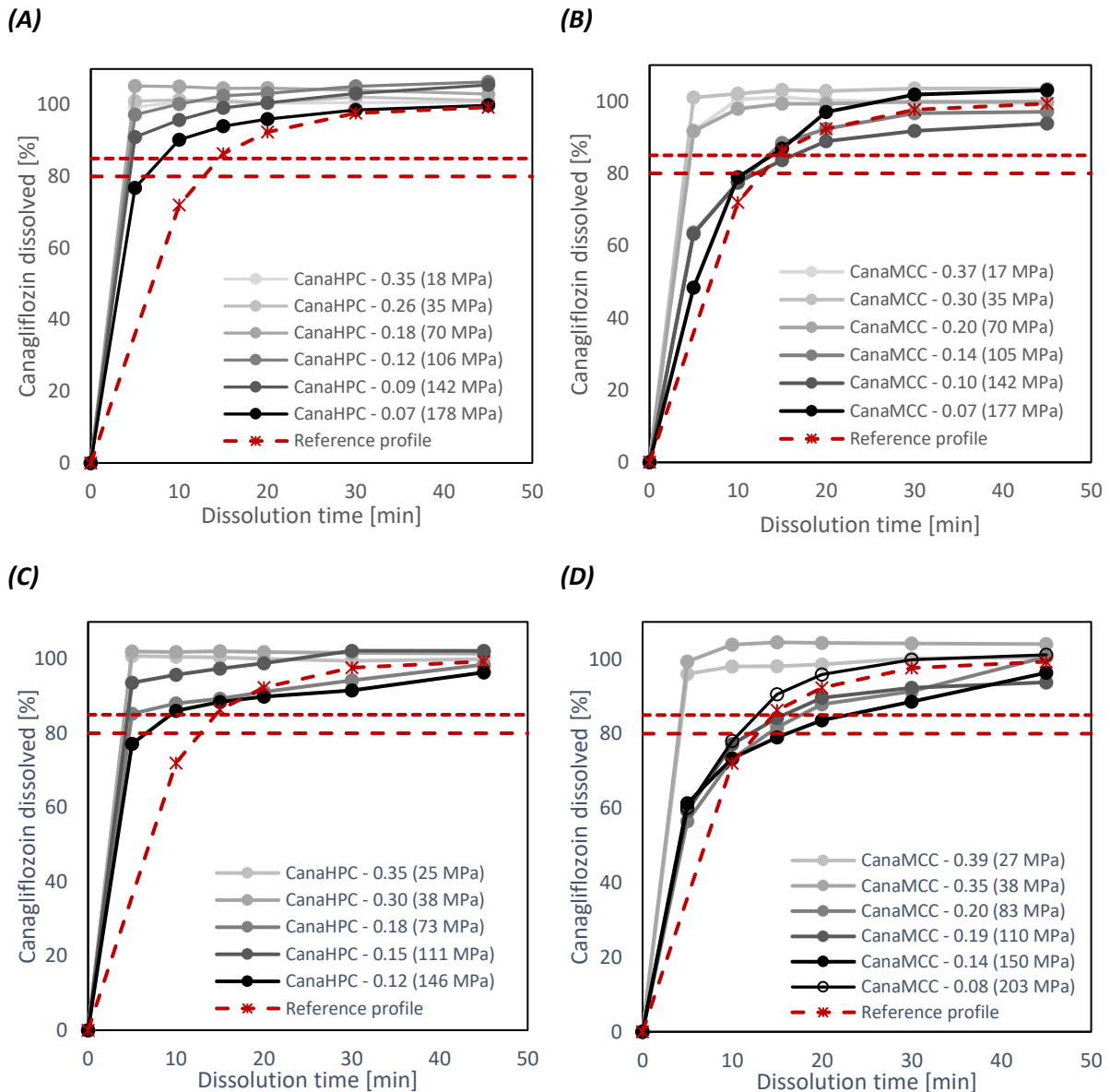


Fig. 11. Dissolution profiles of (A) HPC formulation and (B) MCC formulation both compacted on the Gamlen and dissolution profiles of (C) HPC formulation and (D) MCC formulation both compacted on the Piccola. The porosities are listed after the sample name and the compaction is named in brackets after. The dashed lines indicate the 80/85 % limit of API dissolved by 20/30 minutes.

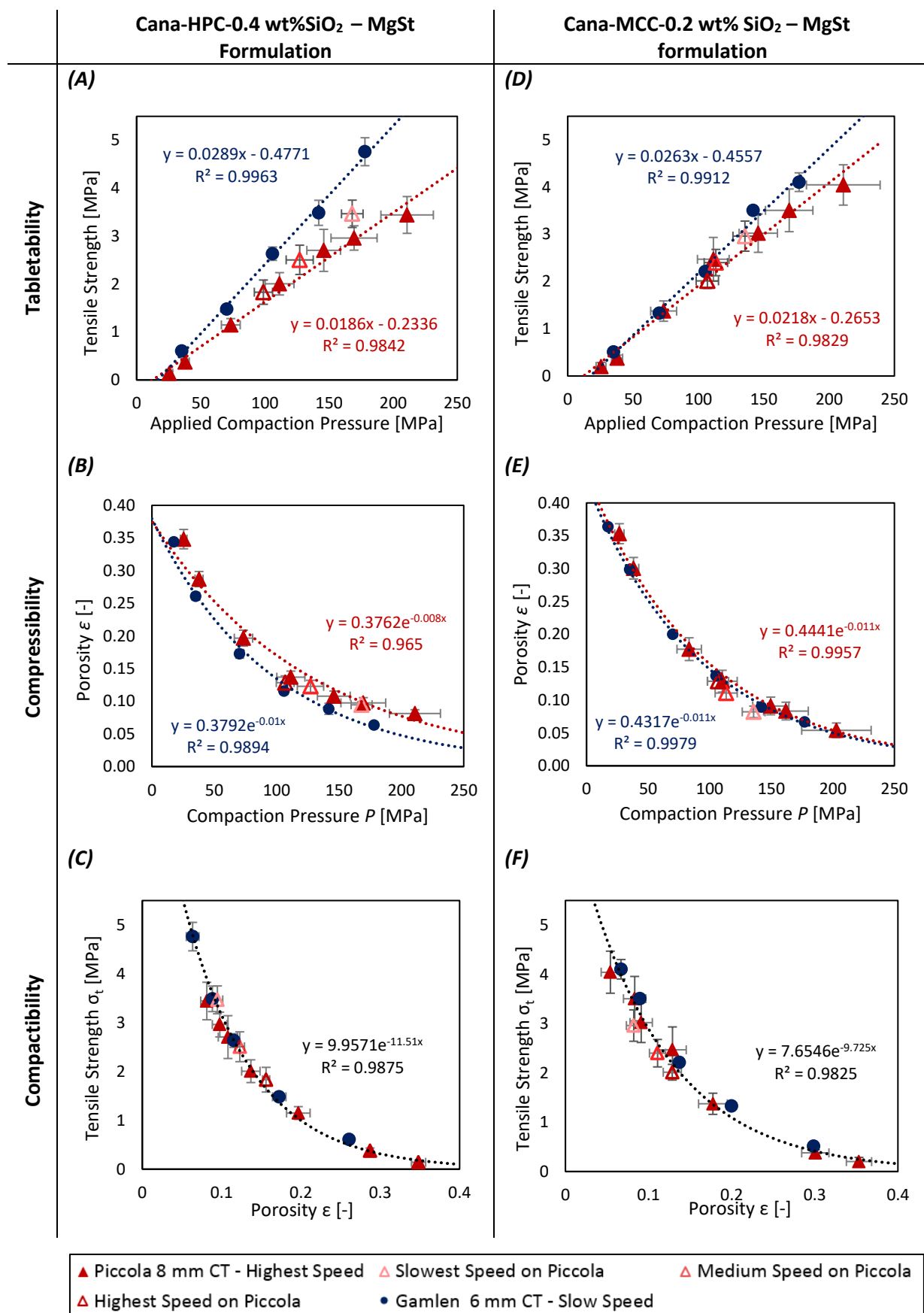
In order to evaluate the tableability, compressibility and compactibility relationships of the formulations, both were tableted on the Gamlen at low speed (1 mm s^{-1}) and at higher speeds on the Piccola rotary tablet press (50 rpm turret speed, $\sim 50 \text{ mm s}^{-1}$ compaction speed). The reason for first compacting on the Gamlen is that the API is expensive to use in large quantities. Small scale compaction allows an understanding of formulations to be developed while sparing material. All relevant responses for a given tablet, including Heckel plots, ejection stress, detachment stress, elastic recovery and tensile strength can be collected from a single compaction and linked on a one-to-one basis with tablet porosity and applied pressure. By compacting tablets at different pressure

level, a full understanding of the key responses is gained and the compaction triangle plots are populated. This is a highly efficient way of assessing formulation performance.

The compaction triangle relationship helps to identify the optimum compaction pressure range to generate OSDs at the desired tensile strength and porosity. Once these are identified the knowledge can be transferred to different equipment. However, it is known, that the tableting speed has an impact on the tabletability and compressibility relationships. Therefore, the compaction triangle relationships need to be reproduced on each equipment. However, the compactibility relationship is generally not sensitive to changes in compaction speeds and can therefore be used as a transferable relationship. Fig. 12 compiles these three relationships of the slow speed on the Gamlen (●) (6 mm/100 mg OSDs) and highest turret speed on the Piccola (▲) (8 mm/200 mg OSDs). To study the impact of the turret speed on the compaction behaviour, three different turret speed settings (Δ) at one fixed die fill setting were tested (Fig. 12). The turret speed settings were 7 rpm ('slowest speed on Piccola'), 27 rpm ('medium speed on Piccola') and 50 rpm ('highest speed on Piccola').

As the compactibility relationship is not affected by varying equipment, tableting speed and tablet size, the optimum tensile strength vs. porosity window could be established. Based on specified required limits on the required tablet crushing force for commercial tablets, the target tensile strength σ_T was calculated to be $2.79 \pm 27\%$ MPa (2.03 to 3.55 MPa) for both formulations. Using the σ_T limits and the determined fitted equation of the compactibility relationship, the optimum porosity was determined as 0.088 to 0.143 and 0.086 to 0.148 for the HPC and MCC formulations, respectively. To control these values in practice, the tablet thickness is used as control parameter. Based on the tablet volume and size, the optimum thickness for round, flat-faced tablets was calculated to be approximately 3.1 – 3.2 mm for 8 mm (200 mg) and 2.7 – 2.9 mm for 6 mm (100 mg) dosage forms. The calculated thickness and the established compaction pressures from the Gamlen tabletability and compressibility relationships were used to quickly establish settings for the Piccola tableting. To approach the work on the Piccola, the die fill needed to be adjusted first to achieve the target weight of 200 mg. This was carried out at the lowest turret speed setting (7 rpm). The fill is controlled by the bottom punch position, which is manually adjusted prior a run. The turret speed was increased to medium turret speed (27 rpm) and then to the highest turret speed (50 rpm). The original set weight of around 200 mg dropped to 195 mg at medium turret speed and to around 190 mg at the highest turret speed for both formulations. The reason for the weight drop is due to the decreased die fill time at higher speeds. The recorded responses were also added to Fig. 12 as open triangle symbols. In order to perform the compaction triangle on the Piccola, the die fill was readjusted to achieve the 200 mg target weight at the highest turret speed. The chosen compaction

pressures were similar to the compaction pressures used on the Gamlen. The compaction triangle plots were generated for the HPC (Fig. 12 (A) – (C)) and MCC formulation (Fig. 12 (D) – (F)).



695 Fig. 12. Overview of the compaction triangle plots for tableability, compressibility and compactibility relationships for HPC formulation (A – C) and MCC formulation (D – F)

The tableability plots shown in Fig. 12 (A) and (D) indicate that strong tablets can be attained at reasonable pressures, which backs up the earlier calculation of low mean yield pressures. However, it is clearly visible that the equipment and tableting speed has an impact on the tableability. The HPC formulation shows quite a significant difference between the Gamlen (●) and the Piccola (▲), but also the initial different speed settings on the Piccola show a reduction in tensile strength at higher turret speeds (Δ). The MCC blend is observed to be less sensitive to tableting speed with a much smaller deviation from results on the Gamlen. Similar observations apply to the compressibility plots (B) and (E). These two relationships indicate that the MCC formulation is less sensitive to compaction speed changes compared to the HPC formulation. The compactibility relationship is scale independent and shows an excellent fit to the Ryshkewitch-Duckworth equation. The HPC formulation shows a higher bonding capacity and theoretical tensile strength at zero porosity. In general, on this basis the HPC blend shows a slightly better performance, but both formulations satisfy the tensile strength requirements near the target porosity of approximately 0.11. Overall, all data points from the three different tablet presses, which operated at different compaction speed and different OSD sizes, fitted to the compactibility relationship, which shows that this is a useful tool for scale-up.

The Piccola also measures the ejection forces. Fig. 13 shows the ejection stresses vs. porosity plots from the compaction triangle runs. Compared to the plots in Fig. 10, which were generated on the Gamlen, the ejection stresses are a significantly higher for the HPC formulation. However, no tableting defects were observed. It should be emphasised that the ejection stress cut-off point of 5 MPa has been specified in the literature for slow compaction speeds. The tablet porosities are in the same range in both the Piccola and Gamlen, so the higher ejection stresses for the HPC formulation on the Piccola are likely due to the much faster ejection speed. Interestingly, similar to the compressibility and tableability data above, the ejection stresses for the MCC formulation seem largely independent of ejection speed. The overall variation of the ejection stresses is much larger for the Piccola data. The reason for this may be due to some variation in the distribution of magnesium stearate within the blend, where tablets with less magnesium stearate could lead to higher ejection stresses. Also, a variation in the applied force between individual punches results in tablets with slightly different porosities, which can also influence ejection stress.

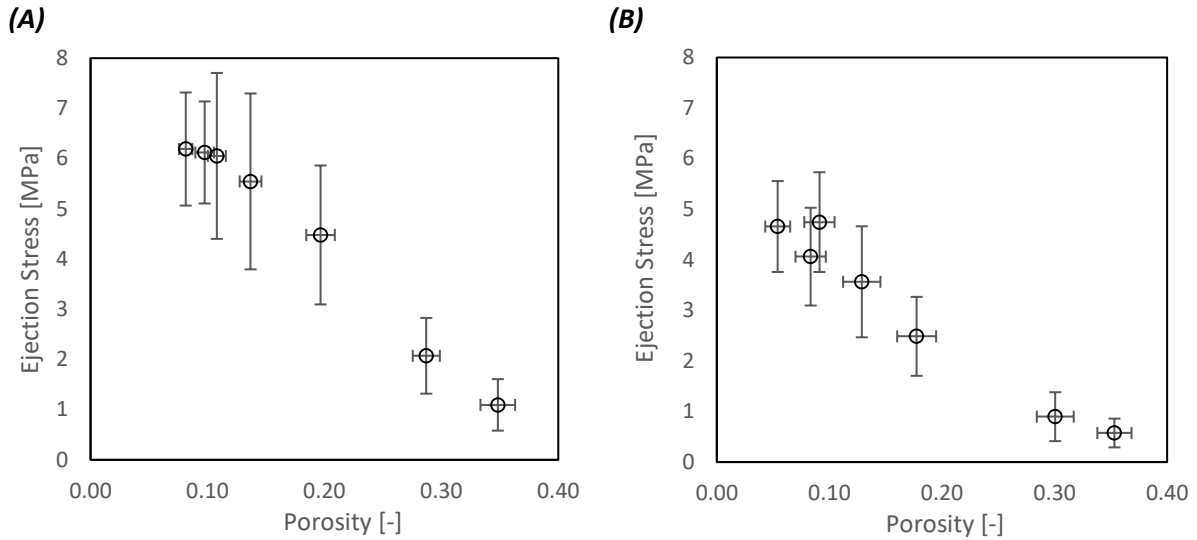


Fig. 13. Ejection stresses vs. porosity of the HPC formulation (A) and MCC formulation (B) performed on the Piccola at 50 rpm turret speed, under different compaction pressures. The variation in porosity and ejection stress within the batches is indicated with error bars.

730

Table 5 summarises the most important tableting values at the target properties for the HPC (A) and MCC (B) formulation. Both formulations lie in the target ranges of thickness, porosity and tensile strength. The tablet weight variation is slightly more inconsistent in MCC formulation, whereby the MCC formulation requires lower compaction pressures and also has much lower ejection stresses

735 than the HPC formulation.

Table 5 Values of the most suitable target runs for the HPC (A) and MCC (B) formulation run on the Piccola at the highest turret speed setting

(A) HPC formulation						(B) MCC formulation					
<i>P</i>	<i>h</i>	ϵ	σ_t	<i>ES</i>	<i>m</i>	<i>P</i>	<i>h</i>	ϵ	σ_t	<i>ES</i>	<i>m</i>
[MPa]	[mm]	[-]	[MPa]	[MPa]	[mg]	[MPa]	[mm]	[-]	[MPa]	[MPa]	[mg]
146	3.19	0.11	2.70	6.05	203.0	110	3.10	0.13	2.47	3.56	193.2
<i>RSD%</i>	0.8	7.1	16.2	27.3	1.5	<i>RSD%</i>	0.6	12.9	18.8	30.8	2.2
170	3.16	0.10	2.96	6.12	203.7	150	3.08	0.09	3.02	4.75	200.0
<i>RSD%</i>	1.0	8.2	8.6	16.6	1.7	<i>RSD%</i>	0.6	14.8	13.4	20.8	1.7

740

4 Conclusion

This work shows that a high dosage formulation for direct compression can be developed and its behaviour can be characterised and predicted using the described systematic approach. This approach is material sparing and allows a relatively quick formulation development. In this work, two optimised formulations were developed for the API canagliflozin at a 51 wt% loading and were successfully scaled-up from a slow compacting single punch compaction simulator to an R&D rotary tablet press. The compactibility relationship was shown to be a good scale-up factor, with consistent behaviour across different compaction speeds and equipment. During the formulation development, several learnings will facilitate faster formulation development and transfer of products currently manufactured batch wise to continuous direct compression processes. The generated material database and the systematic protocol will help to quickly categorise new materials and formulations. Maintained properly, and continuously expanded to include new materials and responses, the database serves as a shortcut to rapid decision making on potential formulations. The compressibility% was shown to be a more reliable predictor of the flow behaviour of interest than the flow function. However, the need to consider different measures of flowability, relevant to different unit operations is emphasised. The compaction triangle relations are found to be vital for formulation development with the key compaction variables of porosity, tensile strength and compaction pressure being characterised. Added to this, an understanding of the influence of compaction speed on the formulation is vital for successful scale-up. Other measures such as bulk density, mean yield pressure and particle size distribution (d90 and d50) are found to be predictable based on the blend composition, but further research is needed to advance their use in formulation development.

5 Acknowledgements

This publication has emanated from research supported in part by a research grant from Science Foundation Ireland (SFI) 'Modelling of Multi-Phase Transport Processes to Enable Automation in Manufacturing, (MOMEntUM)' and is co-funded under the European Regional Development Fund under Grant Number 14/SP/2750, in partnership with Janssen Pharmaceuticals.

6 References

- [1] Parikh, D.M. ed., 2016. Handbook of pharmaceutical granulation technology. CRC Press.
- [2] Patel, S., Kaushal, A.M., Bansal, A.K., 2006. Compression Physics in the Formulation Development of Tablets. *Critical Reviews in Therapeutic Drug Carrier Systems* 23, 1–66.
doi:10.1615/CritRevTherDrugCarrierSyst.v23.i1.10
- [3] Gohel, M.C., Jogani, P.D., 2005. A review of co-processed directly compressible excipients. *Journal of Pharmacy and Pharmaceutical Sciences*.
- [4] Järvinen, M.A., Paaso, J., Paavola, M., Leiviskä, K., Juuti, M., Muzzio, F., Järvinen, K., 2013a. Continuous direct tablet compression: Effects of impeller rotation rate, total feed rate and drug content on the tablet properties and drug release. *Drug Development and Industrial Pharmacy* 39, 1802–1808. doi:10.3109/03639045.2012.738681
- [5] Van Snick, B., Holman, J., Cunningham, C., Kumar, A., Vercruysse, J., De Beer, T., Remon, J.P., Vervaet, C., 2017a. Continuous direct compression as manufacturing platform for sustained release tablets. *International Journal of Pharmaceutics* 519, 390–407.
doi:10.1016/j.ijpharm.2017.01.010
- [6] Reynolds, G.K., Campbell, J.I., Roberts, R.J., 2017. A compressibility based model for predicting the tensile strength of directly compressed pharmaceutical powder mixtures. *International Journal of Pharmaceutics* 531, 215–224. doi:10.1016/j.ijpharm.2017.08.075
- [7] Rogers, A., Ierapetritou, M., 2014. Challenges and opportunities in pharmaceutical manufacturing modeling and optimization. *Computer Aided Chemical Engineering* 34, 144–149.
doi:10.1016/B978-0-444-63433-7.50015-8
- [8] Sinka, I.C., Schneider, L.C.R., Cocks, A.C.F., 2004. Measurement of the flow properties of powders with special reference to die fill. *International Journal of Pharmaceutics* 280, 27–38.
doi:10.1016/j.ijpharm.2004.04.021
- [9] Schneider, L.C.R., Sinka, I.C., Cocks, A.C.F., 2007. Characterisation of the flow behaviour of pharmaceutical powders using a model die-shoe filling system. *Powder Technology* 173, 59–71.
doi:10.1016/j.powtec.2006.11.015
- [10] York, P., 1979. A consideration of experimental variables in the analysis of powder compaction behaviour. *Journal of Pharmacy and Pharmacology* 31, 244–246. doi:10.1111/j.2042-7158.1979.tb13487.x
- [11] Wang, Y., Li, T., Muzzio, J., Glasser, B., 2017. Predicting feeder performance based on material flow properties. *Powder Technology* 308, 135–148. doi:10.1016/j.powtec.2016.12.010.
- [12] Wu, C.Y., Dihoru, L., Cocks, A.C.F., 2003. The flow of powder into simple and stepped dies. *Powder Technology* 134, 24–39. doi:10.1016/S0032-5910(03)00130-X

- 805 [13] Liu, L.X., Marziano, I., Bentham, A., Lister, J., White, E.T., Howes, T., 2008. Effect of particle
properties on the flowability of ibuprofen powders. *International Journal of Pharmaceutics* 362,
109–117. doi:10.1016/j.ijpharm.2008.06.023
- [14] Koynov, S., Glasser, B., Muzzio, F., 2015. Comparison of three rotational shear cell testers:
Powder flowability and bulk density. *Powder Technology* 283, 103–112.
810 doi:10.1016/j.powtec.2015.04.027
- [15] Wang, Y., Snee, R.D., Meng, W., Muzzio, F.J., 2016. Predicting flow behavior of pharmaceutical
blends using shear cell methodology: A quality by design approach. *Powder Technology* 294,
22–29. doi:10.1016/j.powtec.2016.01.019
- [16] Capece, M., Silva, K.R., Sunkara, D., Strong, J., Gao, P., 2016. On the relationship of inter-particle
815 cohesiveness and bulk powder behavior: Flowability of pharmaceutical powders. *International
Journal of Pharmaceutics* 511, 178–189. doi:10.1016/j.ijpharm.2016.06.059
- [17] Peeters, E., De Beer, T., Vervaet, C., Remon, J.P., 2015. Reduction of tablet weight variability by
optimizing paddle speed in the forced feeder of a high-speed rotary tablet press. *Drug
Development and Industrial Pharmacy* 41, 530–539. doi:10.3109/03639045.2014.884121
- 820 [18] Wu, C.Y., Best, S.M., Bentham, A.C., Hancock, B.C., Bonfield, W., 2005. A simple predictive
model for the tensile strength of binary tablets. *European Journal of Pharmaceutical Sciences*
25, 331–336. doi:10.1016/j.ejps.2005.03.004
- [19] Wu, C.Y., Best, S.M., Bentham, A.C., Hancock, B.C., Bonfield, W., 2006. Predicting the tensile
strength of compacted multi-component mixtures of pharmaceutical powders. *Pharmaceutical*
825 *Research* 23, 1898–1905. doi:10.1007/s11095-006-9005-6
- [20] Garr, J.S.M., Rubinstein, M.H., 1991. An investigation into the capping of paracetamol at
increasing speeds of compression. *International Journal of Pharmaceutics* 72, 117–122.
doi:10.1016/0378-5173(91)90049-T
- [21] Sinha, T., Bharadwaj, R., Curtis, J., Hancovk, B., Wassgren, C., 2010. Finite element analysis of
830 pharmaceutical tablet compaction using a density dependent material plasticity model. *Powder
Technology* 202, 46–54. doi:10.1016/j.powtec.2010.04.001
- [22] Yohannes, B., Gonzalez, M., Abebe, A., Sprockel, O., Nikfar, F., Kang, S., Cuitino, A.M., 2015. The
role of fine particles on compaction and tensile strength of pharmaceutical powders. *Powder
Technology* 274, 372–378. doi:10.1016/j.powtec.2015.01.035
- 835 [23] Thoorens, G., Krier, F., Rozet, E., Carlin, B., Evrard, B., 2015. Understanding the impact of
microcrystalline cellulose physicochemical properties on tabletability. *International Journal of
Pharmaceutics* 490, 47–54. doi:10.1016/j.ijpharm.2015.05.026

- [24] Schmidtke, R., Schröder, D., Menth, J., Staab, A., Braun, M., Wagner, K.G., 2017. Prediction of solid fraction from powder mixtures based on single component compression analysis. International Journal of Pharmaceutics 523, 366–375. doi:10.1016/j.ijpharm.2017.03.054
- [25] Paul, S., Taylor, L.J., Murphy, B., Krzyzaniak, J., Dawson, N., Mullarney, M., Meenan, P., Sun, C.C., 2017. Powder properties and compaction parameters that influence punch sticking propensity of pharmaceuticals. International Journal of Pharmaceutics 521, 374–383. doi:10.1016/j.ijpharm.2017.02.053
- [26] Järvinen, K., Hoehe, W., Järvinen, M., Poutiainen, S., Juuti, M., Borchert, S., 2013b. In-line monitoring of the drug content of powder mixtures and tablets by near-infrared spectroscopy during the continuous direct compression tableting process. European Journal of Pharmaceutical Sciences 48, 680–688. doi:10.1016/j.ejps.2012.12.032
- [27] Ervasti, T., Simonaho, S.P., Ketolainen, J., Forsberg, P., Fransson, M., Wikström, H., Folestad, S., Lakio, S., Tajarobi, P., Abrahmsén-Alami, S., 2015. Continuous manufacturing of extended release tablets via powder mixing and direct compression. International Journal of Pharmaceutics 495, 290–301. doi:10.1016/j.ijpharm.2015.08.077
- [28] Lakio, S., Tajarobi, P., Wikström, H., Fransson, M., Arnehed, J., Ervasti, T., Simonaho, S.P., Ketolainen, J., Folestad, S., Abrahmsén-Alami, S., 2016. Achieving a robust drug release from extended release tablets using an integrated continuous mixing and direct compression line. International Journal of Pharmaceutics 511, 659–668. doi:10.1016/j.ijpharm.2016.07.052
- [29] Simonaho, S.P., Ketolainen, J., Ervasti, T., Toiviainen, M., Korhonen, O., 2016. Continuous manufacturing of tablets with PROMIS-line - Introduction and case studies from continuous feeding, blending and tableting. European journal of pharmaceutical sciences : official journal of the European Federation for Pharmaceutical Sciences 90, 38–46. doi:10.1016/j.ejps.2016.02.006
- [30] Engisch, W.E., Muzzio, F.J., 2014. Loss-in-Weight Feeding Trials Case Study: Pharmaceutical Formulation. Journal of Pharmaceutical Innovation 10, 56–75. doi:10.1007/s12247-014-9206-1
- [31] Engisch, W.E., Muzzio, F.J., 2015. Feedrate deviations caused by hopper refill of loss-in-weight feeders. Powder Technology 283, 389–400. doi:10.1016/j.powtec.2015.06.001
- [32] Sun, C.C., Hou, H., Gao, P., Ma, C., Medina, C., Alvarez, F.J., 2009. Development of a high drug load tablet formulation based on assessment of powder manufacturability: Moving towards quality by design. Journal of Pharmaceutical Sciences 98, 239–247. doi:10.1002/jps.21422
- [33] Tye, C.K., Sun, C., Amidon, G.E., 2005. Evaluation of the effects of tableting speed on the relationships between compaction pressure, tablet tensile strength, and tablet solid fraction. Journal of Pharmaceutical Sciences 94, 465–472. doi:10.1002/jps.20262

- [34] United States Pharmacopeia, 2017. Chapter <1062> Tablet Compression Characterization, USP40-NF35.
- [35] Jain, H., Khomane, K.S., Bansal, A.K., 2014. Implication of microstructure on the mechanical
875 behaviour of an aspirin–paracetamol eutectic mixture. *CrystEngComm* 16, 8471–8478.
doi:10.1039/C4CE00878B
- [36] Ryshkewitch, E., 1953. Compression Strength of Porous Sintered Alumina and Zirconia: 9th
Communication to Ceramography. *Journal of the American Ceramic Society* 36, 65–68.
doi:10.1111/j.1151-2916.1953.tb12837.x
- 880 [37] Discussion of Ryshkewitch Paper by Winston Duckworth, 1953. *Journal of the American Ceramic
Society* 36, 68–68. doi:10.1111/j.1151-2916.1953.tb12838.x
- [38] Heckel, R.W., 1961. Density-Pressure Relationships in Powder Compaction. *Transactions of the
Metallurgical Society of AIME* 221, 671–675.
- [39] Kawakita, K., Lüdde, K.H., 1971. Some considerations on powder compression equations.
885 *Powder Technology* 4, 61–68. doi:10.1016/0032-5910(71)80001-3
- [40] Adams, M.J., Mullier, M.A., Seville, J.P.K., 1994. Agglomerate strength measurement using a
uniaxial confined compression test. *Powder Technology* 78, 5–13. doi:10.1016/0032-
5910(93)02777-8
- [41] Zhao, J., Burt, H.M., Miller, R.A., 2006. The Gurnham equation in characterizing the
890 compressibility of pharmaceutical materials. *International Journal of Pharmaceutics* 317, 109–
113. doi:10.1016/j.ijpharm.2006.02.054
- [42] Sun, C.C., 2010. Setting the bar for powder flow properties in successful high speed tableting.
Powder Technology 201, 106–108. doi:10.1016/j.powtec.2010.03.011
- [43] Shi, L., Chattoraj, S., Sun, C.C., 2011. Reproducibility of flow properties of microcrystalline
895 cellulose - Avicel PH102. *Powder Technology* 212, 253–257. doi:10.1016/j.powtec.2011.05.024
- [44] Hirschberg, C., Sun, C.C., Rantanen, J., 2016. Analytical method development for powder
characterization. *Journal of Pharmaceutical and Biomedical Analysis* 128, 462–468.
doi:10.1016/j.jpba.2016.06.014
- [45] Pitt, K.G., Webber, R.J., Hill, K.A., Dey, D., Gamlen, M.J., 2015. Compression prediction accuracy
900 from small scale compaction studies to production presses. *Powder Technology* 270, 490–493.
doi:10.1016/j.powtec.2013.10.007
- [46] Pitt, K.G., Heasley, M.G., 2013. Determination of the tensile strength of elongated tablets.
Powder Technology 238, 169–175. doi:10.1016/j.powtec.2011.12.060
- [47] Osamura, T., Takeuchi, Y., Onodera, R., Kitamura, M., Takahashi, Y., Tahara, K., Takeuchi, H.,
905 2016. Characterization of tableting properties measured with a multi-functional compaction

instrument for several pharmaceutical excipients and actual tablet formulations. *International Journal of Pharmaceutics* 510, 195–202. doi:10.1016/j.ijpharm.2016.05.024

[48] Osamura, T., Takeuchi, Y., Onodera, R., Kitamura, M., Takahashi, Y., Tahara, K. and Takeuchi, H., 2017. Formulation design of granules prepared by wet granulation method using a multi-functional single-punch tablet press to avoid tableting failures. *Asian Journal of Pharmaceutical Sciences*.

[49] Laiko, S., Vajna, B., Farkas, I. Salokangas, H., Marosi, G., 2013. Challenges in detecting magnesium stearate distribution in tablets. *American Association of Pharmaceutical Scientists PharmSciTech* 14, 435–444. doi:10.1208/s12249-01309927-3.

[50] United States Pharmacopeia. Chapter <1174> Powder Flow, USP29-NF24, 2017.

[51] Fell, J.T., Newton, J.M., 1970. Determination of tablet strength by the diametrical compression test. *Journal of Pharmaceutical Sciences* 59, 688–691. doi:10.1002/jps.2600590523

[52] Zinchuk, A.V., Mullarney, M.P., Hancock, B.C., 2004. Simulation of roller compaction using a laboratory scale compaction simulator. *International Journal of Pharmaceutics* 269, 403–415. doi:10.1016/j.ijpharm.2003.09.034

[53] Houlzer, A.W., Sjogren, J., 1977. Comparison of methods for evaluation of friction during tableting. *Drug Development and Industrial Pharmacy* 3, 23–37. doi:10.3109/03639047709055603

[54] Gamlen, M., 2017. Analysis of PROSOLV® EASYtab with added ascorbic acid. Report by Gamlen Instruments. Report number GTL/17/10.

[55] Newton, J.M., Rowley, G., Fell, J.T., Peacock, D.G., Ridgeway, K., 1971. Computer analysis of the relation between tablet strength and compaction pressure. *Journal of Pharmacy and Pharmacology* 23, 195S–201S. doi:10.1111/j.2042-7158.1971.tb08789.x

[56] Sonnergaard, J.M., 2006. Quantification of the compactibility of pharmaceutical powders. *European Journal of Pharmaceutics and Biopharmaceutics* 63, 270–277. doi:10.1016/j.ejpb.2005.10.012

[57] Michrafy, A., Michrafy, M., Kadiri, M.S., Dodds, J.A., 2007. Predictions of tensile strength of binary tablets using linear and power law mixing rules. *International Journal of Pharmaceutics* 333, 118–126. doi:10.1016/j.ijpharm.2006.10.008

[58] United States Pharmacopeia. Chapter <701> Disintegration, USP29-NF24, 2670.

[59] Huang, Z., Scicolone, J.V., Gurumuthy, L., Davé, R.N., 2015. Flow and bulk density enhancements of pharmaceutical powders using a conical screen mill: A continuous dry coating device. *Chemical Engineering Science* 125, 209–224. doi:10.1016/j.ces.2014.05.038

- 940 [60] Han, X., Ghoroi, C., Davé, R., 2013. Dry coating of micronized API powders for improved dissolution of directly compacted tablets with high drug loading. *International Journal of Pharmaceutics* 442, 74–85. doi:10.1016/j.ijpharm.2012.08.004
- [61] United States Pharmacopeia, 2017. Chapter <1062> Tablet Compression Characterization, USP40-NF35.